Fe
13 Cr
8 Ni
2 Mo

PH13-8Mo

1 GENERAL

This alloy is a precipitation-hardenable martensitic stainless steel combining excellent corrosion resistance with exceptionally high strength and hardness. PH13-8Mo was developed during the 1960's. It is normally made by vacuum-induction melting plus consumable-electrode vacuum-arc remelting. It was developed specifically for use in large cross-section parts which require yield strength up to about 220 ksi and good ductility properties irrespective of grain orientation. Toughness in the transverse direction is achieved by compositional control to prevent formation of delta ferrites, by lower carbon content to minimize grain-boundary carbide precipitation, and by double vacuum melting to reduce alloy segregation. The M_S temperature is near room temperature. It has good fabrication properties. Heat treatment consists of a solution treatment followed by aging. Cooling rates from the solution temperature are not critical, allowing heavy sections to be air cooled. Strengthening is effected both by transformation to martensite during cooling from the solution temperature and by precipitation of NiAl intermetallic phase during aging. Long-time exposure at moderately elevated temperatures causes microstructural instability which results in decreased fracture toughness. The alloy has good resistance to general corrosion and to stress corrosion.

PH13-8Mo is generally supplied in the solution-treated condition, ready for fabrication and subsequent age hardening by the user. It can also be supplied in the hardened and the overaged conditions for cold heading or forging if desired. Applications include forgings, cold-headed and machined fasteners, aircraft parts, shuttle rocket-engine mounts, launch-structure parts, nuclear-reactor components, landing-gear parts, pins and lock washers, high-performance shafting, and petrochemical components requiring stress-corrosion resistance combined with high strength. PH13-8Mo is an alloy designation of Armco Steel Corporation.

1.01 **Commercial Designation**

PH13-8Mo stainless steel.

1.02 **Alternate Designation**

UNS 13800.

1.03 **Specifications**

1.031 AMS specifications, Table 1.031.

1.04 **Composition**

1.041 Specified composition, Table 1.041.

1.05 **Heat Treatment**

1.051 The alloy is supplied from the mill in Condition A and can be heat treated at any one of several temperatures to develop a wide range of properties. In Condition A the alloy can be joined to PH14-8Mo, PH15-7Mo or 17-7PH and the entire assembly hardened by three-step heat treatments compatible with the latter grades. For brazed assemblies the steel can be heat treated to satisfactory strength levels using the braze-cycle heat treatment as defined in 1.055. After hot working, brazing, welding, or other treatments that change the metallurgical structure, PH13-8Mo should be reheat-treated to get full design properties (20).

1.052 Condition A. Solution treated 1685 to 1715 F, oil quenched or air cooled below 60 F. Solution treating time should be long enough to assure that the steel is heated thoroughly through the section. Bar and wire items can be effectively heat treated in continuous furnaces. In batch-type furnaces, it is recommended that parts be held at the solution temperature 15 to 30 minutes to assure uniformity.

1.053 Aging treatments, Table 1.053.

1.054 Additional heat-treated conditions (see Table 3.0215).

1.055 Braze-cycle heat treatment (BCHT) condition: 1700 F, 1 hour, cool to 1000 F in 1 hour plus 8 hours at -110 F plus age.

1.056 PH13-8Mo can be satisfactorily heat treated in air-atmosphere furnaces. Inert atmospheres such as argon are often used for aging heat treatment or braze-cycle heat treatments. Controlled reducing atmospheres, such as cracked ammonia, may cause nitriding and are not recommended. In practice, parts are usually fabricated from material in Condition A and only a low-temperature aging treatment in air is required thereafter (22). Solution treatment (1700 F) in molten salt is not recommended because of the danger of carburization and/or intergranular penetration.

1.06 **Hardness**

1.061 Typical hardness of bar in various heat-treated conditions, Table 1.061.

1.062 Effect of solution temperature on the hardness of solution treated-and-aged bar, Figure 1.062.

1.063 Maximum hardening and strengthening are obtained in PH13-8Mo by aging at about 980 F after solution treating at 1650 or 2010 F, as shown in Figures 1.064 and 3.0212. (The standard solution-treating temperature is 1700 F.) In the solution treated-and-quenched condition, the alloy is completely martensitic. Subsequent aging of this martensitic structure in the temperature range 840 to 1070 F leads to finely distributed spherical particles of NiAl precipitate, identified by X-ray diffraction. The lattice mismatch ratio between the matrix and precipitate is very low (less than 0.002). The NiAl precipitate particles, which have a mean radius of 50 Å after aging for 4 hours at 980 F, remain fully coherent with the matrix even after considerable coarsening. Small quantities also of fine cuboidal austenite phase form by reversion on aging at temperatures above 930 F. At aging temperatures higher than 980 F, the amount of austenite phase becomes significant and the austenite particles coarsen rapidly. A major fraction of the observed increase in the flow stress of the aged alloy over that of the solution-treated alloy arises from the presence of the NiAl precipitate. The mechanisms involved include coherency hardening associated with lattice mismatch strains between the matrix and the NiAl precipitate

Fe
13 Cr
8 Ni
2 Mo

PH13-8Mo

particles, modulus hardening resulting from the difference in shear moduli between the matrix and precipitate, and order hardening due to the ordered nature of the precipitate. In addition, the fine austenite particles which form in the martensite matrix contribute significantly toward strengthening the aged alloy (24).

1.064 Effects of aging for 1 or 4 hours on hardness of solution-treated bar, Figure 1.064.

1.065 Effects of aging for 2 hours on hardness of solution-treated bar, Figure 1.065.

1.066 Cold work is seen in Figure 1.067 to first increase and then decrease the hardness of solution-annealed bar. In contrast, the bar data in Table 1.068 indicate constant hardness with increasing cold work after an initial hardness increase. The reason for these differences is not known.

1.067 Effects of cold work on hardness, Figure 1.067.

1.068 Effect of cold work on hardness of bar in various conditions, Table 1.068.

1.069 Effect of aging temperature and time on hardness of cold-worked bar, Table 1.069.

1.07 **Forms and Conditions Available**
Bar, wire, plate, and forging billets in Condition A in hardened conditions, or in an overaged condition.

1.08 **Melting and Casting Practice**
Vacuum-induction melting plus consumable-electrode vacuum-arc remelting (designated VIM + VAR) (3).

1.09 **Special Considerations**

1.091 The fracture toughness of this alloy is good in heavy sections at room temperature and above but decreases rapidly at temperatures below 0 F (see crack strength, Figures 3.03713 and 3.03714). Heavy sections exhibit negligible directionality of tensile properties (see Tables 2.0313, 2.0314, 3.0215, and Figure 3.0218). Fracture toughness also is essentially independent of orientation (see Tables 3.02721 and 3.03722). In common with other alloys of this class, the impact-energy and fracture toughness decrease as a result of long-time exposure to moderately elevated temperature (see Figure 3.0333).

1.092 The resistance to general corrosion of PH13-8Mo exceeds that of Types 410 and 431, and is approximately equal to 17-4PH. Like other precipitation-hardening stainless steels, its level of general corrosion resistance is greatest in the fully hardened condition and decreases slightly as the aging temperature is increased (3). The alloy is the most stress-corrosion resistant of the PH stainless steels (3). See also 2.03.

1.093 Fatigue properties for smooth and notched specimens are independent of orientation (see Figures 3.053, 3.054, and 3.055).

1.094 The highest strength levels in this alloy are obtained by cold working prior to precipitation hardening.

2 PHYSICAL PROPERTIES AND ENVIRONMENTAL EFFECTS

2.01 **Thermal Properties**

2.011 Melting range, 2560 to 2680 F.

2.012 Phase changes. Austenite above about 1500 F, M_S is approximately 250 F but will vary some with composition and can be below room temperature. However, in most cases the martensite transformation is practically complete below 70 F. Aging precipitates intermetallic compounds.

2.0121 Time-temperature transformation diagrams.

2.013 Thermal conductivity, Table 2.013.

2.014 Thermal expansion.

2.0141 Thermal expansion, Figure 2.0141.

2.0142 Dilatometer curve indicating dimensional changes and transformation temperatures for Condition A, Figure 2.0142.

2.015 Specific heat, 0.11 Btu/lb F.

2.016 Thermal diffusivity.

2.02 **Other Physical Properties**

2.021 Density, Table 2.021.

2.022 Electrical properties.

2.0221 Electrical resistivity, Table 2.0221.

2.023 Magnetic properties.

2.0231 Magnetic permeability, Table 2.0231.

2.024 Emittance.

2.025 Damping capacity.

2.03 **Chemical Environments**

2.031 The resistance to general corrosion of PH13-8Mo approaches that of 17-4PH. This is indicated by laboratory immersion tests in both strongly oxidizing and reducing media, as well as by atmospheric exposure. In all heat-treated conditions the alloy exhibits very little rusting after 500 hours exposure to 5 percent salt fog at 95 F. Like other precipitation-hardening stainless steels, its level of general corrosion resistance is greatest in the fully hardened condition and decreases slightly as the aging temperature is increased. PH13-8Mo is the most stress-corrosion resistant of the hardenable stainless steels. It offers higher useful mechanical properties than any other ferrous-base material under extreme environmental conditions (3). Its resistance to stress-corrosion cracking increases as a function of increased aging temperature (see Tables 2.0311 and 2.0317).

2.0311 Stress-corrosion cracking in marine atmosphere, Table 2.0311.

2.0312 Stress-corrosion cracking at Kure Beach in marine atmosphere, Table 2.0312.

2.0313 Stress-corrosion behavior in salt spray and marine atmosphere, Table 2.0313.

2.0314 Stress-corrosion cracking in an NaCl solution, Table 2.0314.

2.0315 Fracture toughness and stress-corrosion values in a 3.5 percent NaCl solution, Table 2.0315.

2.0316 Axial fatigue behavior in seawater and in air, Figure 2.0316.

2.0317 Stress-corrosion cracking in an NaCl-acetic acid-H_2S solution, Table 2.0317.

2.0318 Effects of heat treatment and hardness on stress-corrosion behavior in an NaCl-acetic acid-H_2S solution, Figure 2.0318.

2.0319 Effect of hydrogen charging time on tensile properties, Figure 2.0319.

2.03110 Delayed-failure behavior while being charged with hydrogen, Figure 2.03110.

2.03111	The notched tensile strength is greatly reduced by hydrogen charging. Bar specimens indicated a notched-to-unnotched tensile strength ratio of 1.34, consistent with the high toughness of this alloy. However, after electrolytically charging for 1 hour in 1N H_2SO_4 saturated with CS_2, the tensile-strength ratio for notched charged-to-notched uncharged materials was reduced to 0.39. These results indicate that a considerable reduction in toughness is effected by hydrogen charging. The bar was heat treated to Condition H 950; notched specimens had K_t = 15, 60° circumferential notch, 1.5-mil notch root radius (30).
2.04	**Nuclear Environments**
3	**MECHANICAL PROPERTIES**
3.01	**Specific Mechanical Properties**
3.011	AMS-specified mechanical properties, Table 3.011.
3.012	Producers' guaranteed mechanical properties, Table 3.012.
3.02	**Mechanical Properties at Room Temperature**
3.021	Tension – stress-strain diagrams – tension properties.
3.0211	Stress-strain curves for bar in various aged conditions, Figure 3.0211.
3.0212	True stress-true strain curves for solution-treated and solution treated-and-aged alloy, Figure 3.0212.
3.0213	Typical tensile properties for bar in various heat-treated conditions, Table 3.0213.
3.0214	Effect of solution-treating temperature on the tensile properties of forgings aged at two temperatures, Figure 3.0214.
3.0215	Mechanical properties for various aged conditions, Table 3.0215.
3.0216	Effect of aging and solution-treating temperature on the tensile properties of forgings, Figure 3.0216.
3.0217	Effect of aging temperature on the short transverse tensile properties of forgings, Figure 3.0217.
3.0218	Effect of testing direction on tensile properties of solution treated-and-aged forgings, Figure 3.0218.
3.0219	Effects of cold work on tensile properties, Figure 3.0219.
3.022	Compression – stress-strain diagrams – compression properties.
3.0221	Stress-strain curve in compression for Condition H 1000, Figure 3.0221.
3.0222	Typical compressive yield strengths for bar in various aged conditions, Table 3.0222.
3.023	Impact (see also Tables 3.0215 and 4.0131).
3.0231	Typical impact properties for various heat-treated conditions, Table 3.0231.
3.0232	Effect of solution-treating temperature on the short-transverse impact properties, Figure 3.0232.
3.0233	Effect of aging and solution-treating temperature on impact properties, Figure 3.0233.
3.0234	Effect of solution-treating temperature on the short-transverse impact energy before and after elevated-temperature exposure, Figure 3.0234.
3.024	Bending.
3.025	Torsion and shear.
3.0251	Torsion and shear properties, Table 3.0251.
3.026	Bearing.
3.0261	Bearing properties of sheet in Condition H 1000, Table 3.0261.
3.027	Stress concentration.
3.0271	Notch properties.
3.02711	Effect of surface cracks on crack strength, Figure 3.02711.
3.0272	Fracture toughness.
3.02721	Plane-strain fracture toughness for Condition H 1000, Table 3.02721.
3.02722	Plane-strain fracture toughness in a 3.5 percent NaCl solution (see Table 2.0315).
3.028	Combined properties.
3.03	**Mechanical Properties at Various Temperatures**
3.031	Tension – stress-strain diagrams – tension properties.
3.0311	Stress-strain curves at elevated temperatures for bar in Condition H 1000, Figure 3.0311.
3.0312	Stress-strain curves at room and low temperatures for bar in Condition H 1000, Figure 3.0312.
3.0313	Effect of test temperature on tensile properties of a forging, Figure 3.0313.
3.0314	Effect of test temperature and orientation on the tensile properties of various-size forgings, Table 3.0314.
3.0315	Tensile properties of bar at cryogenic and elevated temperatures, Figure 3.0315.
3.032	Compression – stress-strain diagrams – compression properties.
3.0321	Stress-strain curves for a forging in compression at elevated temperatures, Figure 3.0321.
3.0322	Effect of temperature on compressive yield strength, Figure 3.0322.
3.033	Impact.
3.0331	Typical low-temperature impact energies of bar in various aged conditions, Table 3.0331.
3.0332	Effect of test temperature on impact properties of a forging, Figure 3.0332.
3.0333	Effect of test temperature and exposure temperature on the impact energy of forgings, Figure 3.0333.
3.034	Bending.
3.035	Torsion and shear.
3.036	Bearing.
3.037	Stress concentration.
3.0371	Notch properties.
3.03711	Effect of test temperature on sharp-notch strength of a forging, Figure 3.03711.
3.03712	Effect of stress-concentration factor on tensile and notch properties of bar at room and low temperature, Table 3.03712.
3.03713	Effect of thickness on crack strength of a forging, Figure 3.03713.
3.03714	Effect of test temperature on crack strength of a forging, Figure 3.03714.
3.0372	Fracture toughness.
3.03721	Plane-strain fracture toughness of a forging at low temperature, Table 3.03721.
3.03722	Fracture toughness of various wrought forms at room and cryogenic temperatures, Table 3.03722.
3.038	Combined properties.
3.04	**Creep and Creep-Rupture Properties**
3.041	Time to 0.2 percent creep deformation for bar at elevated temperatures, Figure 3.041.

Fe
13 Cr
8 Ni
2 Mo

PH13-8Mo

Fe
13 Cr
8 Ni
2 Mo

PH13-8Mo

3.042 Time to rupture for bar at elevated temperatures, Figure 3.042.

3.05 **Fatigue Properties** (see also Section 2.0316).

3.051 Effect of stress concentrations on fatigue strength of a forging, Figure 3.051.

3.052 S-N curve for smooth and notched specimens of bar, Figure 3.052.

3.053 S-N curves for longitudinal and transverse smooth and notched specimens from bar at a stress ratio of R = 0.1, Figure 3.053.

3.054 S-N curves for longitudinal and transverse smooth and notched specimens from bar at a stress ratio of R = 0.5, Figure 3.054.

3.055 S-N curves for longitudinal and transverse smooth and notched specimens from bar at a stress ratio of R = -1.0, Figure 3.055.

3.056 S-N curves at elevated temperature for longitudinal smooth and notched specimens from a forging at a stress ratio of R = 0.1, Figure 3.056.

3.057 Fatigue crack-growth rate at room temperature for plate, Figure 3.057.

3.058 Extensive studies of the fatigue-crack-growth behavior of PH13-8Mo (Condition H 1000) were conducted as part of the B-1 bomber design program. The trends observed in these studies with respect to several variables are summarized as follows:

Cyclic frequency – There was no consistently significant effect on varying the frequency from 60 to 360 cpm in low-humidity air or from 6 to 60 cpm in artificial fuel-tank sump residue (water containing 0.12 percent mixed metal chlorides).

Test temperature – Results were inconsistent but suggested that crack-growth rates may be higher at room temperature than at -65 F (see Figure 3.059).

Specimen thickness – There was no consistent difference in crack-growth behavior between 0.5- and 1.0-inch-thick specimens.

R factor – Results ranged from inconsistent effect to significant acceleration when R was increased from 0.08 to 0.3.

Environment – Crack-growth rates were greater in fuel-tank sump residue water (see Figure 3.0510) and in shop cleaning fluid (a trisodium phosphate-type cleaning solution) than in low-humidity air at stress-intensity-factor ranges greater than about 20 ksi $\sqrt{in.}$

Test direction – In general, fatigue-crack-growth rates are slightly greater in the LT direction than in the TL direction. However, in low-humidity air at -65 F, the reverse was observed, as seen by comparison of the data in Figures 3.059 (a) and (b).

Product form – In low-humidity air, no significant differences in crack-growth-rate behavior were observed among forged bar, rolled bar, extrusions, and upset forgings.

The curves shown in Figures 3.059 and 3.0510 are representative of the data observed in PH13-8Mo (31).

3.059 Fatigue crack-growth rate in low-humidity air at low temperatures, (a) LT orientation, and (b) TL orientation, Figure 3.059.

3.0510 Fatigue crack-growth rate in fuel-tank sump water and in air at room temperature, Figure 3.0510.

3.06 **Elastic Properties**

3.061 Poisson's ratio, $\mu = 0.278$.

3.062 Modulus of elasticity.

3.0621 Tensile moduli of bar in various aged conditions, Table 3.0621.

3.0622 Elastic moduli of forged bar in tension and compression at room and elevated temperatures, Figure 3.0622.

3.063 Modulus of rigidity, $G = 11.1 \times 10^3$ ksi (Condition H 950); $G = 10.9 \times 10^3$ ksi (Condition H 1000).

3.064 Tangent modulus.

3.065 Secant modulus.

4 FABRICATION

4.01 **Forming**

4.011 In fabricating PH13-8Mo it is important to keep in mind the low temperature at which the start of transformation to martensite (M_s) and the finish of the martensite transformation (M_f) occur. These temperatures are approximately 250 and 70 F, respectively, but they both vary with composition. Therefore, it is necessary to cool parts in process below 60 F prior to subsequent heat treatments in order to assure grain refinement and good ductility. The following are examples of situations where cooling below 60 F is an important step: (a) cool below 60 F after solution treating prior to applying any of the precipitation-hardening treatments, (b) cool forged parts below 90 F after final forging before solution treating, and (c) cool any weldment below 90 F prior to solution treating (3).

4.012 Forging is the recommended method for forming intricate shapes of this alloy. Forging blanks should be heated uniformly to 2150 to 2200 F and held at temperature for at least 15 minutes before forging. On reheating, they should be soaked thoroughly. After forging, sections should be cooled to below 90 F as stated in Section 4.011. Then, to assure the best condition for the hardening operations, the parts must be re-solution treated to Condition A. In heating for forgings, as in the heat treatment of the alloy, endothermic atmospheres (or other atmospheres that may cause carburization or decarburization) should not be used (3).

4.013 The heat treatment lends itself to a braze cycle (see Section 1.055) which permits brazing heavy sections of this alloy to lighter sections of PH13-8Mo or similar sheet alloys.

4.0131 Tensile and impact properties of forgings subjected to a braze-cycle heat treatment, Table 4.0131.

4.02 **Machining and Grinding**

4.021 General. In Condition A good tool life and surface finish are obtained when machined at speeds 20 to 30 percent lower than those used for 17-4PH

at similar hardness levels. Cutting procedures commonly used for standard chromium-nickel stainless steels are generally satisfactory for PH13-8Mo (3).

4.03 **Joining**

4.031 General. Composition of the alloy is balanced for optimum performance in welding. Low carbon content restricts the hardness of rapidly cooled material and avoids the formation of cracks in weld deposits and heat-affected zones of the base metal, eliminating the need for preheating. It possesses sufficient ductility to prevent stress cracking, thus permitting welding in Condition A or in any heat-treated condition (3).

4.032 Welding process. The weld process most widely used for joining PH13-8Mo is gas tungsten arc (GTA) and the preferred shielding gas is helium. Other processes which can be used include plasma arc and electron beam either with or without the addition of a filler, plus gas metal arc and shielded metal arc where chromium-nickel or nickel-base fillers are to be used (3).

4.033 Filler metal. Choice of weld metal to join the alloy depends on properties required in the weld. When properties comparable to the base metal are required, weld metal of PH13-8Mo can be used. The weld metal can be produced by simple fusion of the base metal, but deposition of WPH13-8Mo filler wire is preferred in order to insure good weld ductility in the hardened condition. The only difference in composition between the base metal and the WPH weld wire is that the latter has a lower aluminum maximum. Austenitic chromium-nickel stainless steel weld metal may be used for joining the alloy when toughness and ductility are the major criteria. When PH13-8Mo is to be joined to a dissimilar material, dilution must be considered. In joining the alloy to a plain-carbon or low-alloy steel, Type 309 stainless should be used. In other dissimilar metal joints when similar thermal-expansion characteristics are needed, the use of a nickel-base alloy weld should be employed (3).

4.034 Effect of heat treatment on the mechanical properties of weldments as a function of plate thickness. Table 4.034.

4.035 The microstructure of PH13-8Mo weld metal at room temperature consists of a small amount of delta ferrite in a martensite-like matrix. The delta ferrite helps maintain high immunity to hot cracking and provides good ductility in the hardened condition (35).

4.036 Fracture-toughness values in butt-weld joints and in weld overlays tested at room temperature range from 79 to 98 ksi $\sqrt{in.}$, as shown in Table 4.037. These values are equal to or greater than 90 percent of the average fracture-toughness values of the parent metal. Differences in fracture-toughness values for HAZ (heat-affected zone) versus weld bead in weld joints, as-welded versus stress-relieved (2 hours, 950 F) weld overlays, and weld overlays versus weld joints were all within replicate scatter ranges (31).

4.037 Fracture toughness of welded material at room and cryogenic temperatures. Table 4.037.

4.04 **Surface Treating**

4.041 The discoloration developed in the final heat treatment can be removed by dipping in a 10 percent HNO_3-2 percent HF pickle solution for 3 minutes maximum. All parts should be passivated in 40 to 60 percent HNO_3 after final cleaning (22).

Fe
13 Cr
8 Ni
2 Mo

PH13-8Mo

REFERENCES

1 AMS 5629C (January 1, 1985).

2 AMS 5840A (July 16, 1979).

3 Armco Steel Corporation, Product Data Bulletin, Armco PH13-8Mo, S-33C (August 1972).

4 Clarke, W. C., Jr., and Garvin, H. W., "Effect of Composition and Section Size on Mechanical Properties of Some Precipitation Hardening Stainless Steels", American Society for Testing Materials, Special Technical Publication No. 369, "Advances in the Technology of Stainless Steels and Related Alloys" (1965).

5 Crossley, F. A., "Research on the Basic Nature of Stress Corrosion for Various Structural Alloys at Room and Elevated Temperature", IIT Research Institute, Air Force Contract AF33(657)-10971 (May 1964).

6 Garvin, H. W., Armco Steel Corporation, Baltimore, Maryland, personal communication with W. F. Brown, Jr. (1964).

7 Alloy Digest, Armco PH13-8Mo (May 1969).

8 Hoenie, A. F., and Roach, D. B., "New Developments in High-Strength Stainless Steels", DMIC Report 223 (January 3, 1966).

9 Humphries, T. S., and Nelson, E. E., "Stress Corrosion Cracking Evaluation of Several Precipitation Hardening Stainless Steels", NASA Technical Memorandum Report No. 53910, Marshall Space Flight Center (September 12, 1969).

10 Carter, C. S., et al., "Stress-Corrosion Properties of High Strength Precipitation-Hardening Stainless Steels in 3.5 Percent Aqueous Sodium Chloride Solution", Boeing Commercial Airplane Group, D6-25219 (February 1970).

11 Garvin, H. W., Armco Steel Corporation, Baltimore, Maryland, personal communication with W. F. Brown, Jr. (1964).

12 "Thick Section Fracture Toughness", ML-TDR 64-236, Boeing North American, Air Force Contract AF 33(657)-11461 (October 1964).

13 Johnson, P. W., Jr., Armco Steel Corporation, Baltimore, Maryland, personal communication with C. F. Hickey, Jr. (February 1973).

14 Bubsey, R. T., and Brown, W. F., Jr., "Crack Toughness Characteristics of Several Alloys for Use in Heavy Sections of High Speed Aircraft", NASA TN D-4998, Lewis Research Center (January 1969).

15 Takas, E. G., Armco Steel Corporation, Baltimore, Maryland, personal communication with C. F. Hickey, Jr. (February 1973).

16 Uchida, J. M., "Evaluation of Armco PH13-8Mo", Boeing Company, Renton, Washington, AD 700 762 (November 19, 1969).

17 Deel, O. L., and Mindlin, H., "Engineering Data on New Aerospace Structural Materials", AFML-TR-72-196, Vol 2 (September 1972).

Fe
13 Cr
8 Ni
2 Mo

PH13-8Mo

18 Shahinian, P., et al., "Fatigue Crack Growth in Selected Alloys for Reactor Applications", *Journal of Materials*, Vol 7, No. 4 (December 1972).

19 AMS 5864 (April 15, 1980).

20 Anonymous, "Good Steels for Tough Weldments", *Welding Design and Fabrication*, Vol 49, No. 2 (February 1976), pp 52–56.

21 "The Effect of Composition and Section Size on Transverse Properties of Precipitation-Hardening Stainless Steels – Part III: PH13-8Mo Stainless Steels", Armco Steel Corporation, Middletown, Ohio, trade literature (1981), 3 pp.

22 "Armco PH13-8Mo", Alloy Digest, Filing Code: SS-224 (May 1969).

23 "Armco Precipitation-Hardening Stainless Steels", Armco Steel Corporation, Baltimore, Maryland, trade literature (1978), 21 pp.

24 Seetharaman, V., Sundararaman, M., and Krisknan, R., "Precipitation Hardening in a PH13-8Mo Stainless Steel", *Materials Science and Engineering*, Vol 47, No. 1 (January 1981), pp 1–11.

25 Asayama, Y., "Precipitation Processes and Notch Tensile Strengths of Precipitation Hardening Stainless Steels", *Journal of the Japan Institute of Metals*, Vol 45, No. 7 (July 1981), pp 731–739.

26 Humphries, T. S., and Nelson, E. E., "Stress Corrosion Cracking Evaluation of Martensitic Precipitation Hardening Stainless Steels", NASA-TM-78257 (January 1980), 34 pp.

27 Tipton, D. G., "Corrosion Fatigue of High Strength Fastener Materials in Seawater", NASA CR-174677 (December 1983), 26 pp.

28 Gaugh, R. R., "Sulfide Stress Cracking of Precipitation Hardening Stainless Steels", *Materials Performance*, Vol 16, No. 9 (September 1977), pp 24–29.

29 Murray, G. T., Honegger, H. H., and Mousel, T., "Hydrogen Embrittlement of PH13-8Mo Stainless Steel – The Effect of Surface Condition", *Corrosion*, Vol 40, No. 4 (April 1984), pp 146–151.

30 Thompson, A. W., "Hydrogen Effects on Fracture of PH13-8Mo Steel", Proceedings of the Fourth International Conference on Fracture", University of Waterloo, Ontario, Canada (June 1977), 6 pp.

31 Ferguson, R. R., and Berryman, R. C., "Fracture Mechanics Evaluation of B-1 Materials. Volume I. Text", AFML TR-76-137-Vol-1 (October 1976).

32 Deel, O., "Collected Enginering Data Sheets (Air Force Data Sheet Program)", AFML TR-78-179 (December 1978).

33 Ferguson, R. R., and Berryman, R. C., "Fracture Mechanics Evaluation of B-1 Materials. Volume II. Fatigue Crack Growth Data", AFML TR-76-137-Vol-2 (October 1976).

34 "Armco PH13-8Mo – Precipitation-Hardening Stainless Steel Bar, Wire, Plate and Forging Billets", Armco Steel Corporation, Baltimore, Maryland, Product Data Bulletin S-33b (May 1970).

35 Espy, H., "Welding the PH Grades", Armco Steel Corporation, Middletown, Ohio, trade literature (1978).

Alloy	PH13-8Mo
AMS Specification	Product Form
5629C	Bars, forgings, rings, extrusions
5840A	Welding wire
5864	Plate

TABLE 1.031. AMS SPECIFICATIONS (1,2,19)

Alloy	PH13-8Mo			
AMS Specification	5629C 5864		5840A	
	Percent		Percent	
Element	Min	Max	Min	Max
Chromium	12.25	13.25	12.25	13.25
Nickel	7.50	8.50	7.50	8.50
Molybdenum	2.00	2.50	2.00	2.50
Aluminum	0.90	1.35	0.90	1.35
Manganese	–	0.10	–	0.10
Silicon	–	0.10	–	0.10
Carbon	–	0.05	–	0.05
Nitrogen	–	0.010	–	0.01
Phosphorus	–	0.010	–	0.008
Sulfur	–	0.008	–	0.010
Oxygen	–	–	–	0.005
Hydrogen	–	–	–	0.0025

TABLE 1.041. SPECIFIED COMPOSITION (1,2,19)

Alloy	PH13-8Mo	
Condition	Aging Temperature, F	Aging Time, hr, Plus AC
RH 950	950(a)	4
H 950	950	4
H 1000	1000	4
H 1025	1025	4
H 1050	1050	4
H 1100	1100	4
H 1150	1150	4
H 1150-M	1400	2
	Followed by	
	1150	4

(a) Refrigerate 2 hours at -100 F within 24 hours after solution annealing and prior to aging.

TABLE 1.053. AGING TREATMENTS (21)

Alloy	PH13-8Mo
Form	1 to 3-inch Bar
Condition	Hardness, HRC
A	33
RH 950	48
H 950	47
H 1000	45
H 1050	43
H 1100	35
H 1150	33
H 1150-M	32

TABLE 1.061. TYPICAL HARDNESS OF BAR IN VARIOUS HEAT-TREATED CONDITIONS (23)

Fe
13 Cr
8 Ni
2 Mo

PH13-8Mo

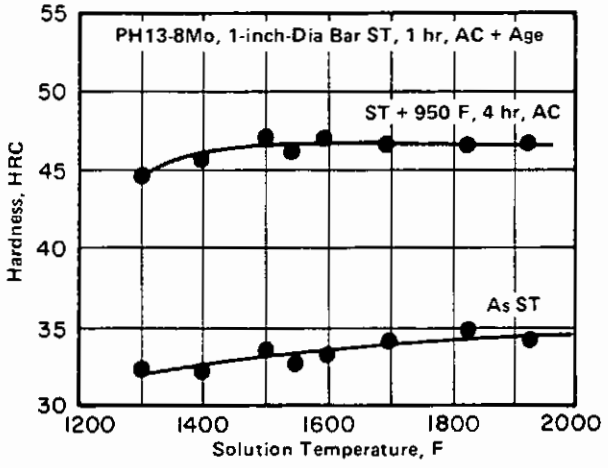

FIGURE 1.062. EFFECT OF SOLUTION TEMPERATURE ON THE HARDNESS OF SOLUTION TREATED-AND-AGED BAR (6)

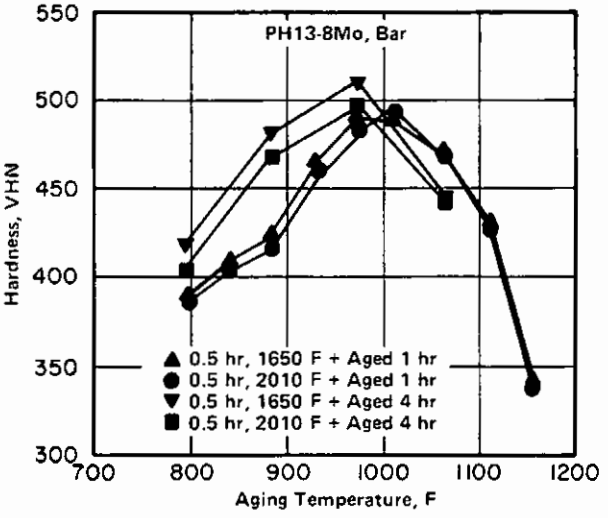

FIGURE 1.064. EFFECTS OF AGING FOR 1 OR 4 HOURS ON HARDNESS OF SOLUTION-TREATED BAR (24)

Fe
13 Cr
8 Ni
2 Mo
PH13-8Mo

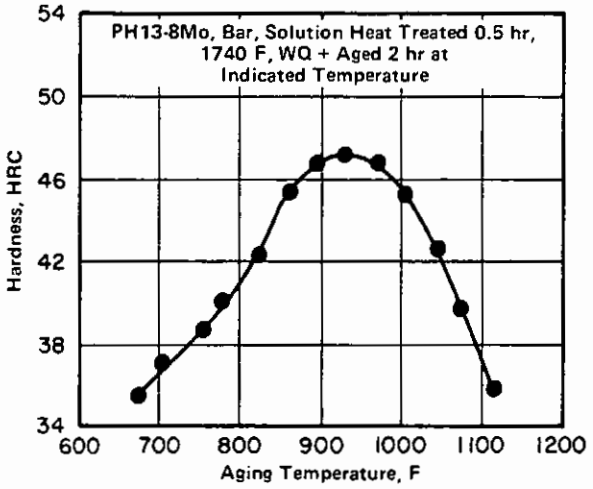

FIGURE 1.065. EFFECTS OF AGING FOR 2 HOURS ON HARDNESS OF SOLUTION-TREATED BAR (25)

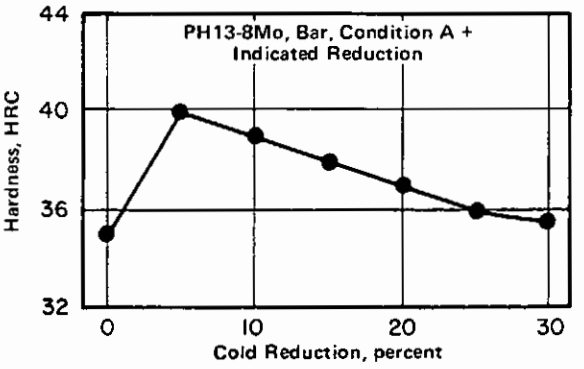

FIGURE 1.067. EFFECTS OF COLD WORK ON HARDNESS (22)

Alloy	13PH-8Mo		
Condition	A	H 900[a]	H 950[a]
Reduction in Diameter (by forging), percent	Hardness, HRC		
0	35	46	45
5	40	48	46
10	40	48	46
15	40	48	46
20	40	47	46
25	40	–	–
30	40	–	–

(a) Fabrication sequence – A + CW + age 4 hours.

TABLE 1.068. EFFECT OF COLD WORK ON HARDNESS OF BAR IN VARIOUS CONDITIONS (3)

Alloy	13PH-8Mo			
Form	0.750-inch-Diameter Bar (Final Diameter)			
Condition	Cold Reduced 10 percent + H 900		Cold Reduced 10 percent + H 1000	
Aging Time, hr	Hardness		Hardness	
1	47	46	47	46
4	48	47	46	46
8	49	48	45	44
16	49	48	44	43

TABLE 1.069. EFFECT OF AGING TEMPERATURE AND TIME ON HARDNESS OF COLD-WORKED BAR (3)

Alloy	PH13-8Mo
Condition	A
Temperature, F	Thermal Conductivity, Btu·ft/hr·ft^2·F
212	8.1
392	9.1
599	10.3
797	11.8
1004	12.7
1112	13.1

Fe
13 Cr
8 Ni
2 Mo
PH13-8Mo

TABLE 2.013. THERMAL CONDUCTIVITY (3)

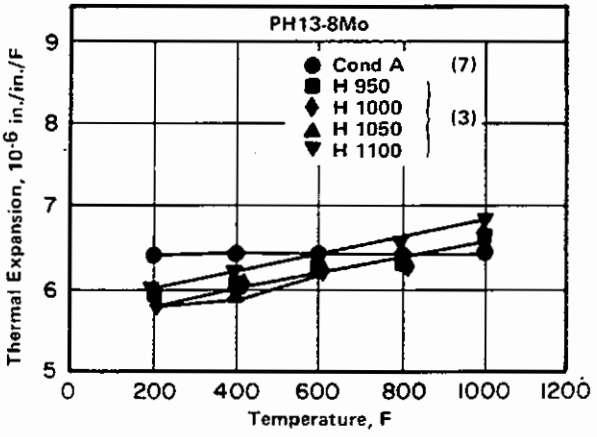

FIGURE 2.0141. THERMAL EXPANSION (3,7)

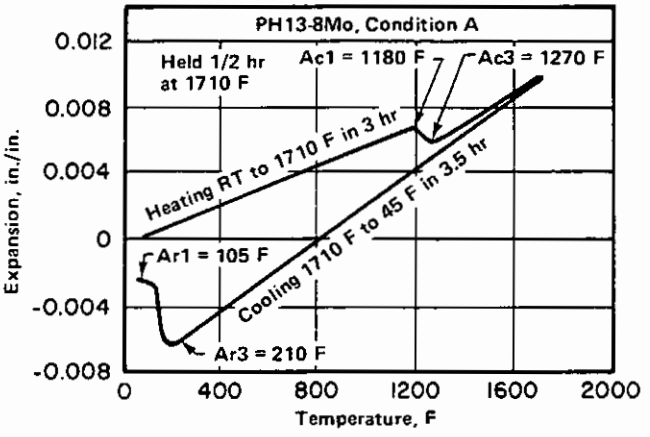

FIGURE 2.0142. DILATOMETER CURVE INDICATING DIMENSIONAL CHANGES AND TRANSFORMATION TEMPERATURES FOR CONDITION A (3)

Alloy	PH13-8Mo	
Condition	A	H 1000
lb/in.^{3}	0.279	0.279
gr/cm^3	7.74	7.76

TABLE 2.021. DENSITY (3)

Alloy	PH13-8Mo
Condition	A
Temperature, F	Electrical Resistivity, μohm-in.
212	40.1
392	41.2
599	41.8
797	42.6
1004	43.0
1112	43.2

TABLE 2.0221. ELECTRICAL RESISTIVITY (3)

Fe
13 Cr
8 Ni
2 Mo
PH13-8Mo

Alloy	PH13-8Mo					
Condition	H 950					
Field Strength, oersteds	10.5	54.7	110.5	164.5	217	264
Permeability	52	127	85	65	53	46

TABLE 2.0231. MAGNETIC PERMEABILITY (15)

Alloy	PH13-8Mo	
Form	0.062-inch Strip	
Condition	Applied Stress[a], ksi	Days to Failure[b] (80-ft lot, Kure Beach)
H 950[c]	204	1 sample failed after 353 days; 1 after 1077 days; 1 NF
	184	1 sample failed after 51 days; 2 NF
	153	1 sample failed after 1077 days; 2 NF
H 1000[c]	199	3 NF
	179	3 NF
	149	3 NF
H 1050[c]	172	3 NF
	155	3 NF
	149	3 NF
Solution treated, welded, aged at 1000 F for 4 hours	195	3 samples failed after 43 days
	176	3 samples failed after 43 days
	146	1 sample failed after 43 days; 1 after 100 days
Solution treated, welded, solution treated and aged at 1000 F for 4 hours	195	3 NF
	176	3 NF
	146	3 NF

(a) Applied stresses were 100, 90, and 75 percent of the 0.2 percent yield strength, using smooth, bent beam specimens tested in the longitudinal direction.
(b) NF indicates no failure in 1405 days' exposure.
(c) Heat treatment includes solution treatment at 1700 F for 15 minutes.

TABLE 2.0311. STRESS-CORROSION CRACKING IN MARINE ATMOSPHERE (3)

Alloy	PH13-8Mo			
Form	0.050-inch Sheet			
Condition	BCHT-900			
	Original Properties		Applied Stress 90 Percent F_{ty}	
Orientation	F_{tu}, ksi	F_{ty}, ksi	Stress, ksi	Days to Failure, (80-ft lot)
Longitudinal	235	215	193	396
Transverse	248	223	201	487

TABLE 2.0312. STRESS-CORROSION CRACKING AT KURE BEACH IN MARINE ATMOSPHERE (8)

Fe
13 Cr
8 Ni
2 Mo
PH13-8Mo

Alloy		PH13-8Mo				
Form		Bar[a]				
		Original Tensile Properties		Applied Tensile Stress, Percent F_{ty}	Ratio of Failures to Number Exposed	
Condition	Orientation	F_{tu}, ksi	F_{ty}, ksi		Salt Spray[b]	Seacoast[c]
H 950	Longitudinal	222	206	75	0/3	–
				100	0/3	–
	Transverse	221	203	75	3/9	1/5
				100	5/12	3/5
H 1000	Longitudinal	205	194	25	–	0/3
				50	0/3	0/3
				75	0/3	–
				100	2/3	–
	Transverse	206	200	25	0/6	0/22
				50	7/45	10/50
				75	12/54	8/34
				100	11/39	0/30
H 1050	Longitudinal	183	172	25	–	0/3
				50	1/3	0/3
				75	1/3	–
	Transverse	183	177	25	0/3	0/17
				50	5/33	0/37
				75	5/33	0/27
				100	2/20	1/19

(a) Average data from seven heats.
(b) 6-month exposure.
(c) 14-month exposure.

TABLE 2.0313. STRESS-CORROSION BEHAVIOR IN SALT SPRAY AND MARINE ATMOSPHERE (26)

Alloy		PH13-8Mo				
Form		10-inch-Diameter Bar				
Test Environment		3.5 percent NaCl				
		Original Properties		Applied Stress		Days to Failure[a]
Condition	Orientation	F_{tu}, ksi	F_{ty}, ksi	ksi	Percent F_{ty}	
H 950	Longitudinal	231	217	163	75	NF
		231	217	196	90	NF
	Transverse	226	211	158	75	NF
		226	211	190	90	NF
H 1000	Longitudinal	222	212	159	75	NF
		222	212	191	90	NF
	Transverse	219	210	158	75	NF
		219	210	190	90	NF

(a) NF denotes no failure after 6 months.

TABLE 2.0314. STRESS-CORROSION CRACKING IN AN NaCl SOLUTION (9)

Fe
13 Cr
8 Ni
2 Mo

PH13-8Mo

Alloy	PH13-8Mo			
Form	4-inch-Square Billet			
Condition	F_{tu}[a], ksi	F_{ty}[a], ksi	Plane-Strain Fracture Toughness[b], K_{Ic}, ksi $\sqrt{in.}$	Plane-Strain Stress-Corrosion Threshold[c], K_{Iscc}, ksi $\sqrt{in.}$
H 950	225	208	73.9	73.9[d,e]

Note: Data average of two longitudinal tests. Specimens heat treated in blank form. Notch specimens were fatigue cracked after heat treatment to produce a precrack approximately 0.1 inch long at the notch root.

(a) 0.25-inch-diameter tension specimen.

(b)

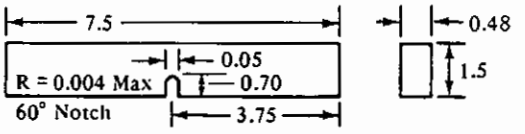

(c)

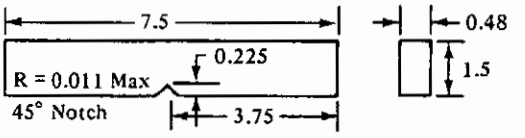

(d) Test environment 3.5 percent NaCl.

(e) No stress-corrosion crack growth at stress-intensity levels exceeding approximately 85 percent K_{Ic}. No crack growth after 1000 hours.

TABLE 2.0315. FRACTURE-TOUGHNESS AND STRESS-CORROSION VALUES IN A 3.5 PERCENT NaCl SOLUTION (10)

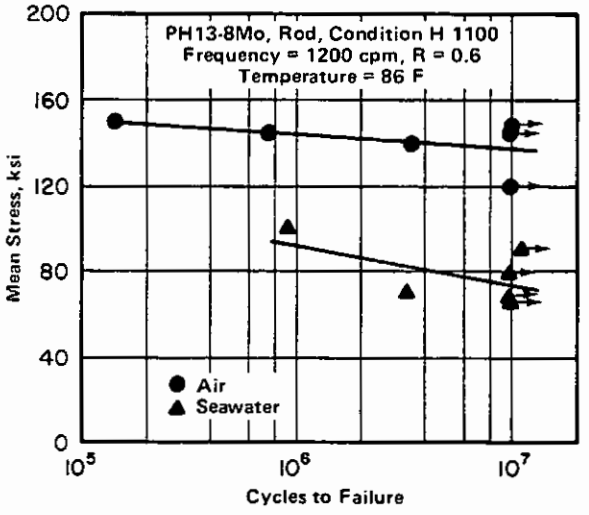

FIGURE 2.0316. AXIAL FATIGUE BEHAVIOR IN SEA-WATER AND IN AIR (27)

Fe
13 Cr
8 Ni
2 Mo
PH13-8Mo

Alloy	PH13-8Mo		
Form	0.250-inch Bar		
Test Environment	6 percent Sodium Chloride Plus 1/2 percent Acetic Acid, Saturated With Hydrogen Sulfide		
Condition	Original F_{ty}, ksi	Applied Stress, ksi	Time to Failure, hr
H 1000	205	100	2.6
		75	3.7
		50	7.4
		25	75.0
H 1100	150	100	8.0
		75	24.0
		50	170.0
		25	>1000

TABLE 2.0317. STRESS-CORROSION CRACKING IN AN NaCl-ACETIC ACID-H_2S SOLUTION (3)

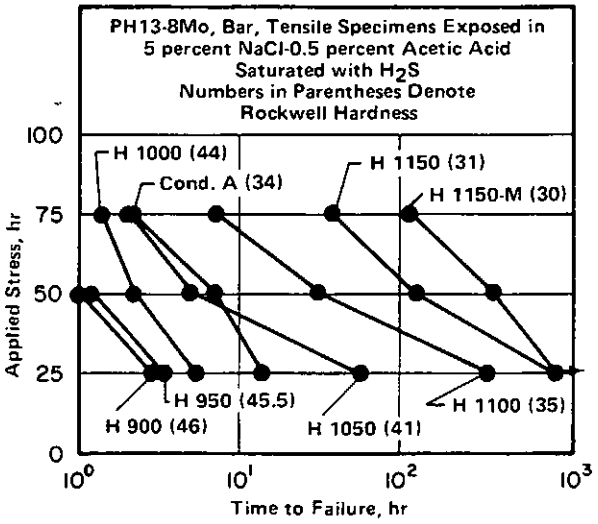

FIGURE 2.0318. EFFECTS OF HEAT TREATMENT AND HARDNESS ON STRESS-CORROSION BEHAVIOR IN AN NaCl-ACETIC ACID-H_2S SOLUTION (28)

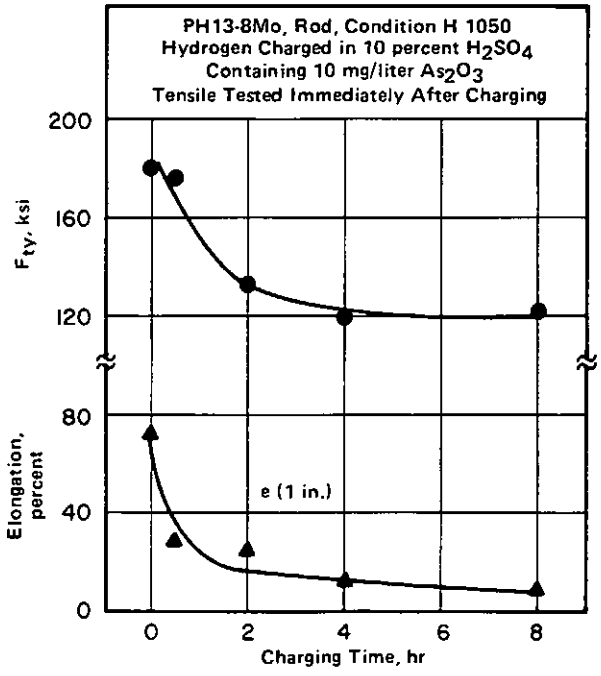

FIGURE 2.0319. EFFECT OF HYDROGEN CHARGING TIME ON TENSILE PROPERTIES (29)

Fe
13 Cr
8 Ni
2 Mo

PH13-8Mo

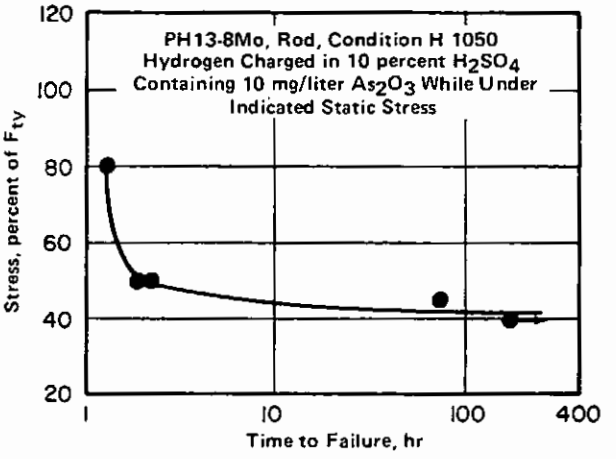

FIGURE 2.03110. DELAYED FAILURE BEHAVIOR WHILE BEING CHARGED WITH HYDROGEN (29)

Alloy	PH13-8Mo								
			Tensile Properties						
AMS Specification	Condition	Specimen Orientation	F_{tu}, ksi Min	F_{tu}, ksi Max	F_{ty}, ksi (Min)	e, percent (Min)(a)	RA, percent (Min)	Hardness Min(b)	Hardness Max
5629C	A	–	–	175(c)	–	–	–	–	363 HB
	H 950	Long.	220	–	205	10	45	45 HRC	–
		Trans.	220	–	205	10	35	45 HRC	–
	H 1000	Long.	205	–	190	10	50	43 HRC	–
		Trans.	205	–	190	10	40	43 HRC	–
	H 1025	Long.	185	–	175	11	50	41 HRC	–
		Trans.	185	–	175	11	45	41 HRC	–
	H 1050	Long.	175	–	165	12	50	40 HRC	–
		Trans.	175	–	165	12	45	40 HRC	–
	H 1100	Long.	150	–	135	14	50	34 HRC	–
		Trans.	150	–	135	14	50	34 HRC	–
	H 1150	Long.	135	–	90	14	50	30 HRC	–
		Trans.	135	–	90	14	50	30 HRC	–
5864	A	–	–	–	–	–	–	–	38 HRC
	H 950	Long.	220	–	205	10	45	45 HRC	–
		Short trans.	220	–	205	10	35	45 HRC	–
	H 1000	Long.	205	–	190	10	50	43 HRC	–
		Short trans.	205	–	190	10	40	43 HRC	–
	H 1025	Long.	185	–	175	11	50	41 HRC	–
		Short trans.	185	–	175	11	45	41 HRC	–
	H 1050	Long.	175	–	165	12	50	40 HRC	–
		Short trans.	175	–	165	12	45	40 HRC	–
	H 1100	Long.	150	–	135	14	50	34 HRC	–
		Short trans.	150	–	135	14	50	34 HRC	–
	H 1150	Long.	135	–	90	14	50	30 HRC	–
		Short trans.	135	–	90	14	50	30 HRC	–

Note: The original AMS documents should be consulted for complete specification details.

(a) 2 inches or 4D.
(b) Not required if tensile-property requirements are met.
(c) Wire only.

TABLE 3.011. AMS-SPECIFIED MECHANICAL PROPERTIES (1,19)

Alloy	PH-13-8Mo (Up to 12-inch Section Size)															
Condition	RH 950		H 950		H 1000		H 1025		H 1050		H 1100		H 1150		H 1150-M	
Orientation	Long.	Trans.	Long.	Trans.	Long.	Trans.	Long.	Trans.	Long.	Trans.	Long.	Trans.	Long.	Trans.	Long.	Trans.
F_{tu}, Min, ksi	220	220	220	220	205	205	185	185	175	175	150	150	135	135	125	125
F_{ty}, Min, ksi	205	205	205	205	190	190	175	175	165	165	135	135	90	90	85	85
e (2 in.), Min, percent	10	10	10	10	10	10	11	11	12	12	14	14	14	14	16	16
RA, Min, percent	45	35	45	35	50	40	50	45	50	45	50	50	50	50	55	55
Hardness, HRC, Min	45	45	45	45	43	43	41	41	40	40	34	34	30	30	26	26
Hardness, BHN, Min	430	430	430	430	400	400	–	–	372	372	313	313	283	283	–	–

Fe
13 Cr
8 Ni
2 Mo
PH13-8Mo

TABLE 3.012. PRODUCERS' GUARANTEED MECHANICAL PROPERTIES (23)

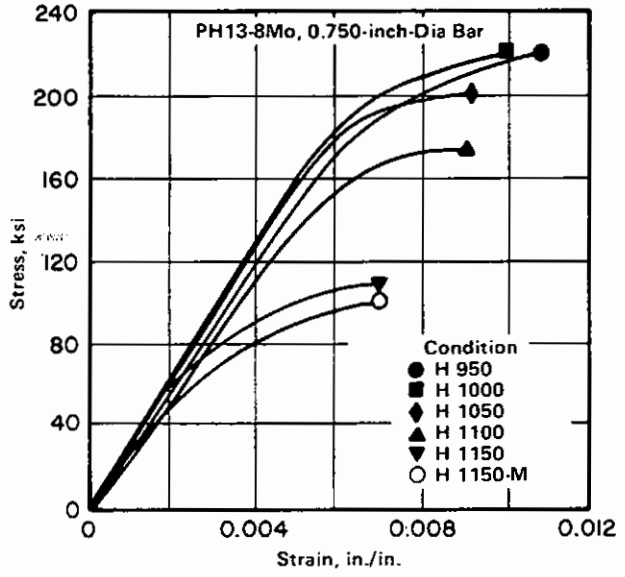

FIGURE 3.0211. STRESS-STRAIN CURVES FOR BAR IN VARIOUS AGED CONDITIONS (13)

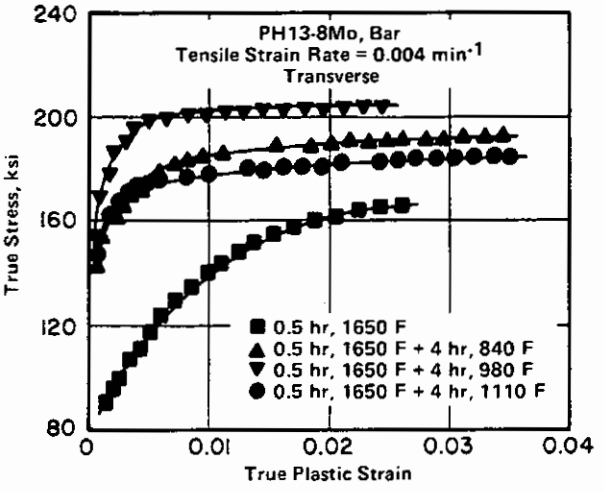

FIGURE 3.0212. TRUE STRESS-TRUE STRAIN CURVES FOR SOLUTION TREATED AND SOLUTION TREATED-AND-AGED ALLOY (24)

Alloy	PH13-8Mo															
Form	1 to 3-inch Bar															
Condition	A		RH 950		H 950		H 1000		H 1050		H 1100		H 1150		H 1150-M	
Orientation	Long.	Trans.	Long.	Trans.	Long.	Trans.	Long.	Trans.	Long.	Trans.	Long.	Trans.	Long.	Trans.	Long.	Trans.
F_{tu}, ksi	160	160	235	235	225	225	215	215	190	190	160	160	145	145	130	130
F_{ty}, ksi	120	120	215	215	210	210	205	205	180	180	150	150	105	105	85	85
e (2 in.), percent	17	17	12	12	12	12	13	13	15	15	18	18	20	20	22	22
RA, percent	65	65	45	35	50	40	55	50	55	55	60	60	63	63	70	70

TABLE 3.0213. TYPICAL TENSILE PROPERTIES FOR BAR IN VARIOUS HEAT-TREATED CONDITIONS (23)

Fe
13 Cr
8 Ni
2 Mo

PH13-8Mo

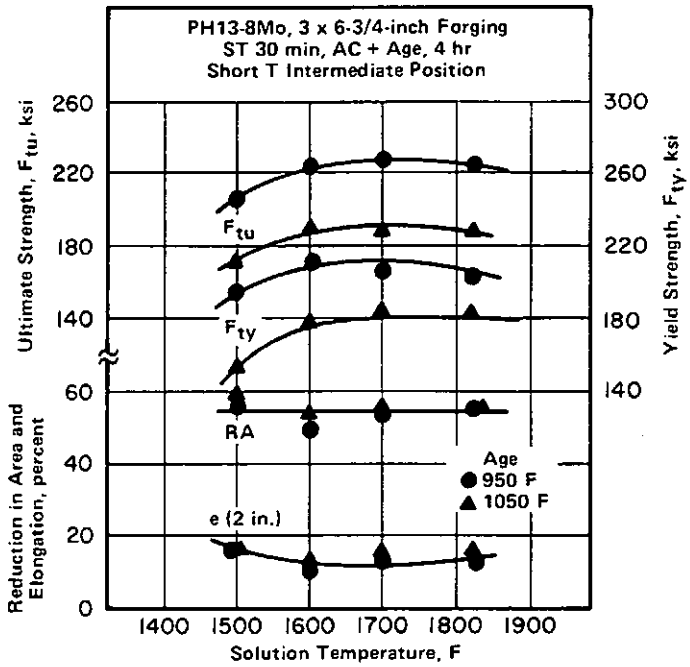

FIGURE 3.0214. EFFECT OF SOLUTION-TREATING TEMPERATURE ON THE TENSILE PROPERTIES OF FORGINGS AGED AT TWO TEMPERATURES (3)

Alloy	PH13-8Mo						
Section Size, in.	Condition[a]	Direction and Location[b]	F_{ty}, ksi	F_{tu}, ksi	e (4 x D), percent	RA, percent	IE Charpy V, ft-lb
9 by 9	A 950	LI	196	218	14	37	–
		TI	201	220	13	31	–
		TC	190	213	14	33	–
3 by 8	A 950	LI	188	214	16	66	18
		LCT	198	220	14	63	–
		STC	193	218	14	53	–
3 by 8	A 1000	LI	188	217	16	66	50
	A 1050	LI	187	195	15	69	111
	A 1100	LI	162	173	18	72	149
	ORH 950	LI	204	225	14	66	28
		STC	200	223	13	61	–

Note: 1825 F is not the recommended solution temperature; data are included for comparison purposes only.

(a) A 950 – 1825 F, 1/2 hr, AC + 950 F, 1 hr, AC
A 1000 – 1825 F, 1/2 hr, AC + 1000 F, 1 hr, AC
A 1050 – 1825 F, 1/2 hr, AC + 1050 F, 1 hr, AC
A 1100 – 1825 F, 1/2 hr, AC + 1100 F, 1 hr, AC
ORH 950 – 1150 F, 4 hr, AC + 1700 F, 1 hr, AC + -100 F, 8 hr + 950 F, 1 hr, AC.
(b) LI = longitudinal intermediate; TC = transverse center; STC = short transverse center.

TABLE 3.0215. MECHANICAL PROPERTIES FOR VARIOUS AGED CONDITIONS (4)

Fe
13 Cr
8 Ni
2 Mo

PH13-8Mo

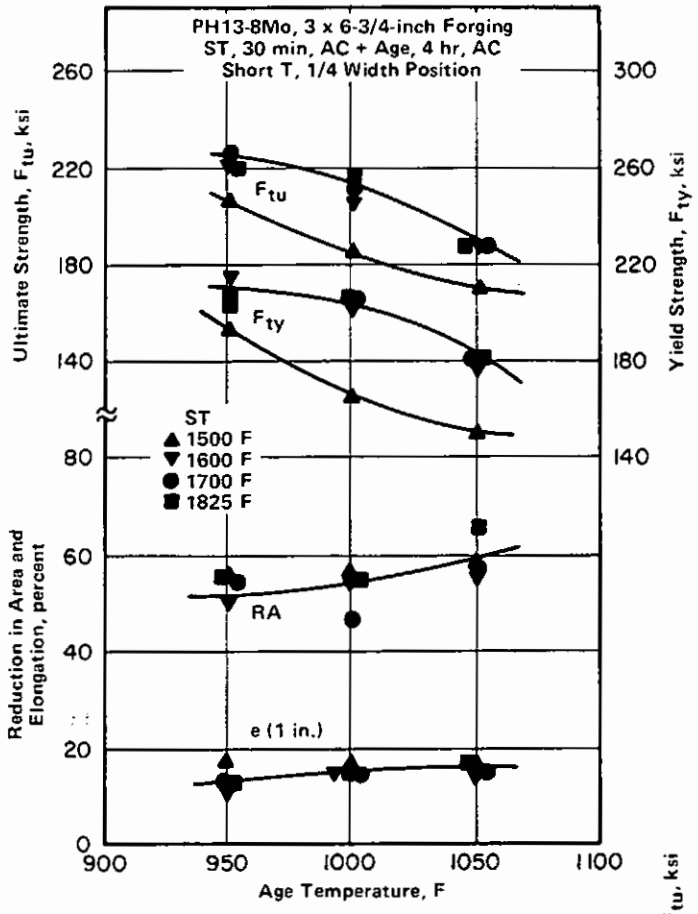

FIGURE 3.0216. EFFECT OF AGING AND SOLUTION-TREATING TEMPERATURE ON THE TENSILE PROPERTIES OF FORGINGS (11)

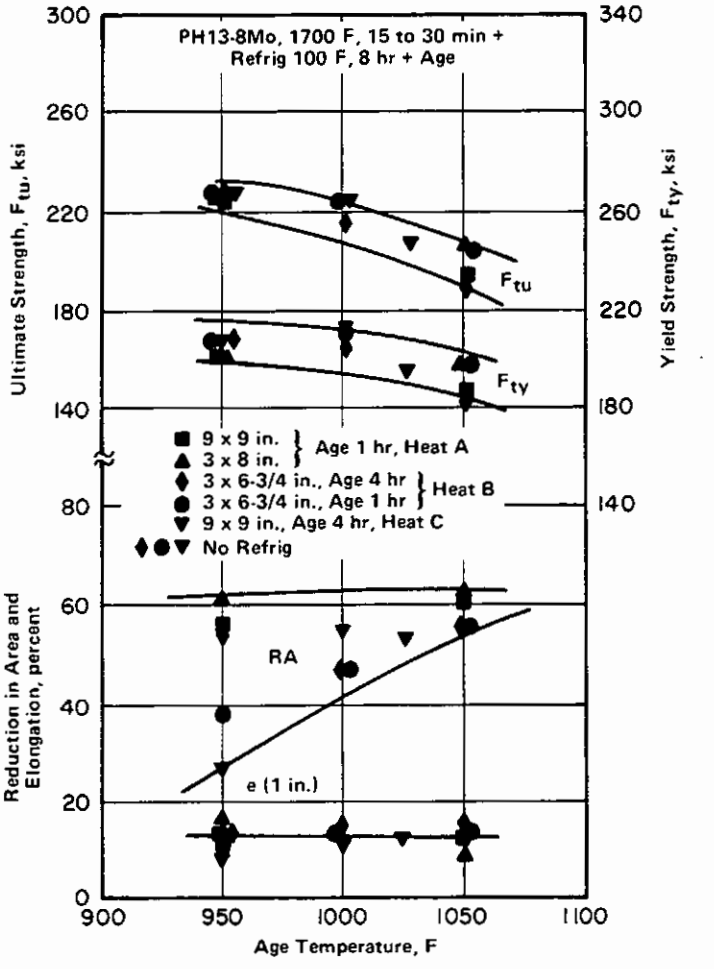

FIGURE 3.0217. EFFECT OF AGING TEMPERATURE ON THE SHORT TRANSVERSE TENSILE PROPERTIES OF FORGINGS (11,12)

Fe
13 Cr
8 Ni
2 Mo

PH13-8Mo

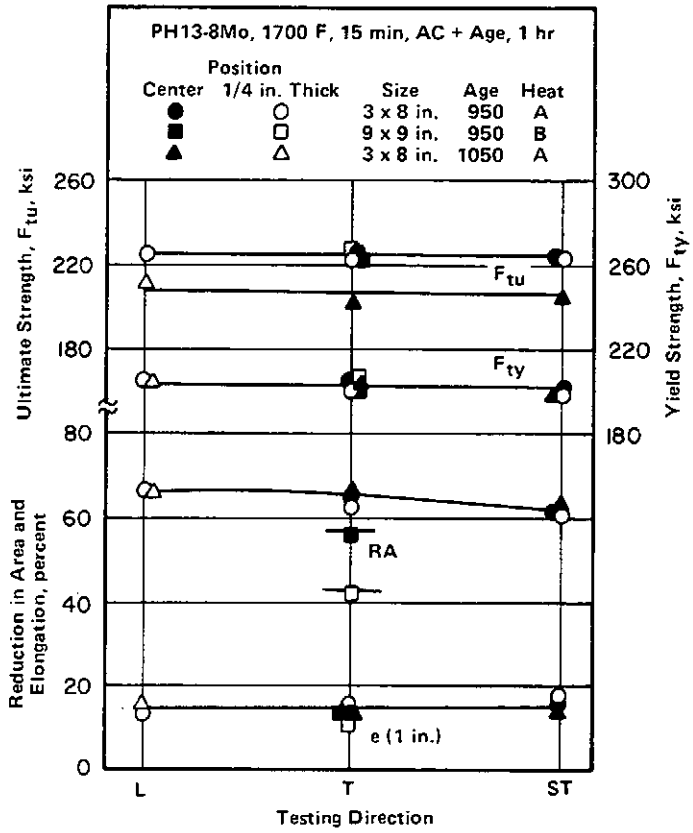

FIGURE 3.0218. EFFECT OF TESTING DIRECTION ON TENSILE PROPERTIES OF SOLUTION TREATED-AND-AGED FORGINGS (11)

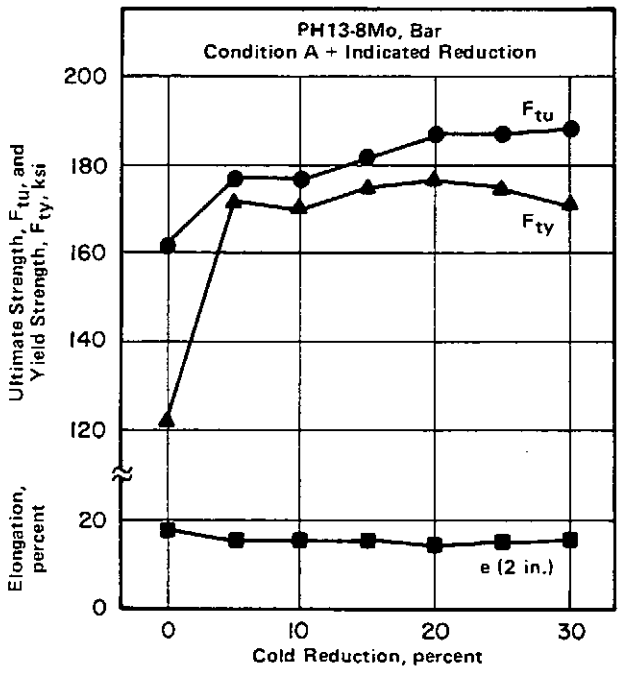

FIGURE 3.0219. EFFECTS OF COLD WORK ON TENSILE PROPERTIES (22)

Fe
13 Cr
8 Ni
2 Mo

PH13-8Mo

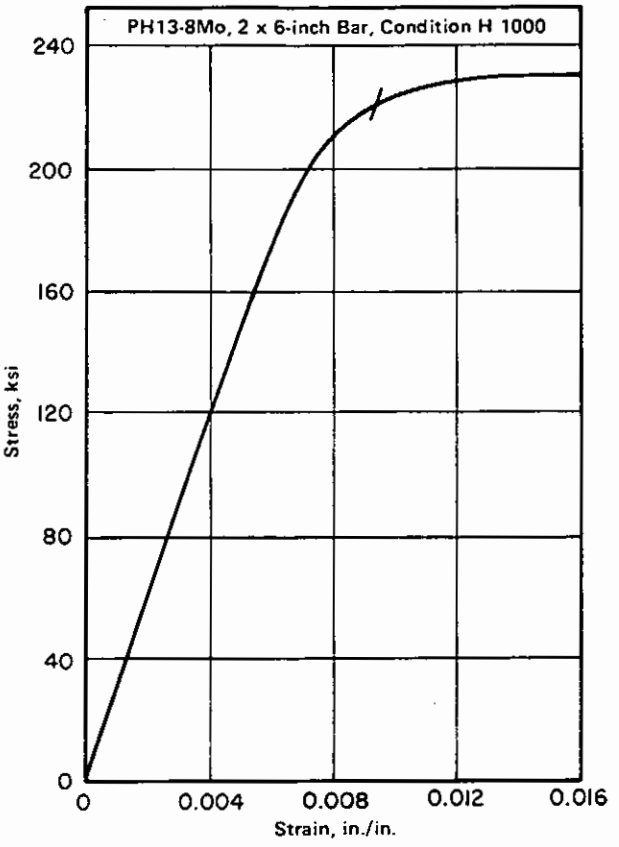

FIGURE 3.0221. STRESS-STRAIN CURVE IN COMPRESSION FOR CONDITION H 1000 (13)

Alloy	PH13-8Mo		
Form	7/8-inch-Diameter Bar		
Condition	H 950	H 1000	H 1050
F_{cy}, ksi			
0.2 percent	220	224	198
0.02 percent	181	196	174

TABLE 3.0222. TYPICAL COMPRESSIVE YIELD STRENGTHS FOR BAR IN VARIOUS AGED CONDITIONS (3)

Alloy	PH13-8Mo	
Form	1 to 3-inch Bar	
	Impact Energy, ft-lb[a]	
Condition	Longitudinal	Transverse
A	60	40
RH 950	20	10
H 950	20	15
H 1000	30	20
H 1050	50	30
H 1100	60	40
H 1150	80	60
H 1150-M	120	80

(a) Charpy V-notch.

TABLE 3.0231. TYPICAL IMPACT PROPERTIES FOR VARIOUS HEAT-TREATED CONDITIONS (23)

Fe
13 Cr
8 Ni
2 Mo

PH13-8Mo

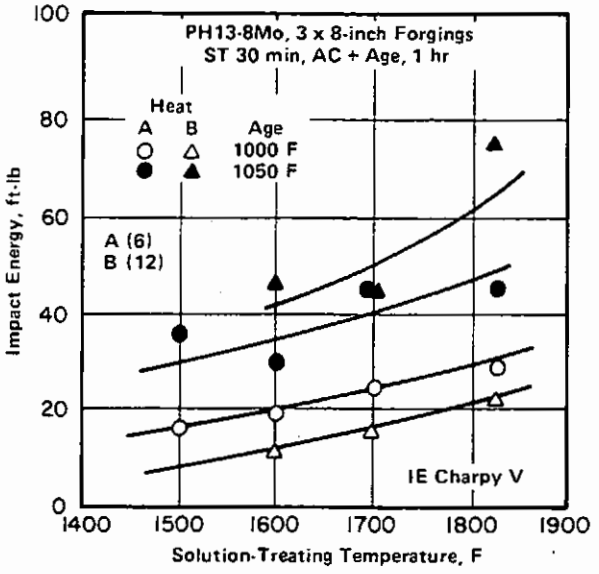

FIGURE 3.0232. EFFECT OF SOLUTION-TREATING TEMPERATURE ON SHORT-TRANSVERSE IMPACT PROPERTIES (6,12)

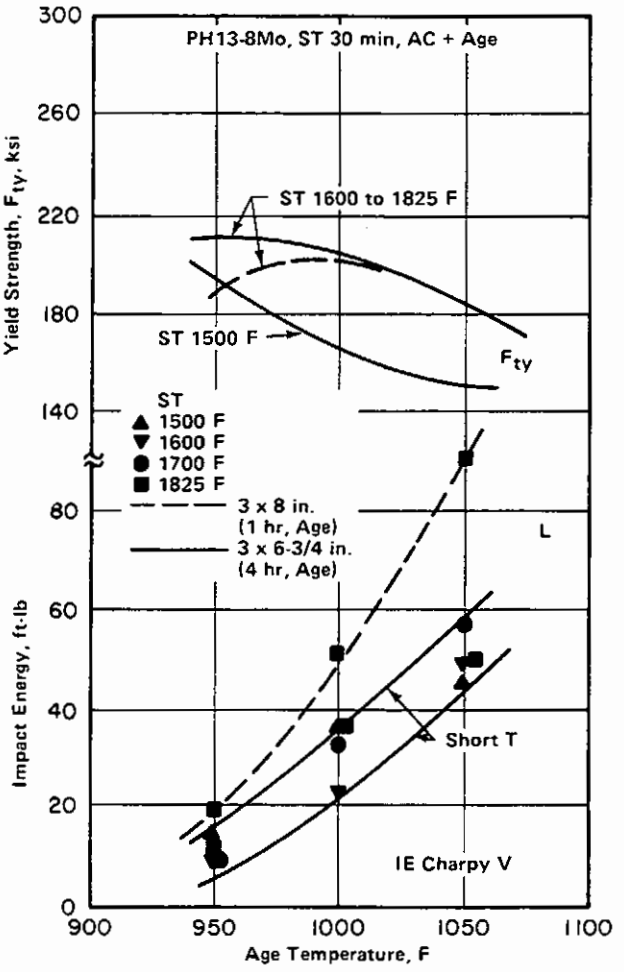

FIGURE 3.0233. EFFECT OF AGING AND SOLUTION-TREATING TEMPERATURE ON IMPACT PROPERTIES (6)

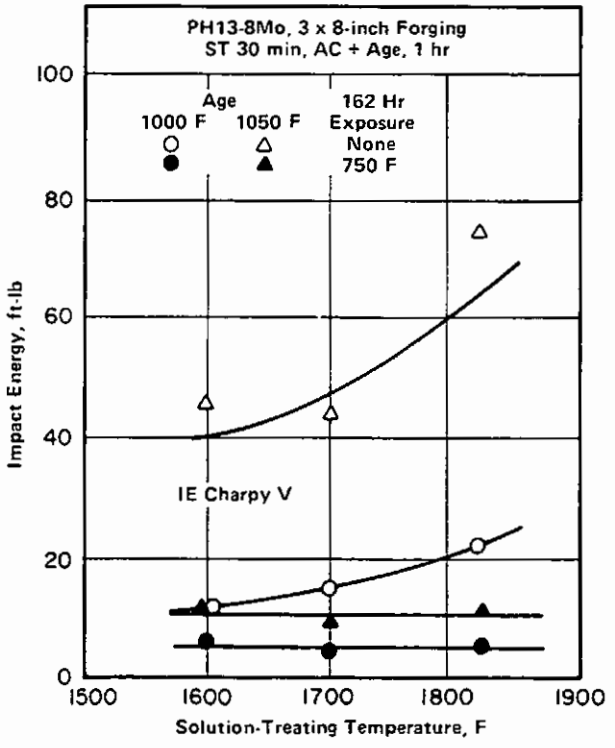

FIGURE 3.0234. EFFECT OF SOLUTION-TREATING TEMPERATURE ON SHORT-TRANSVERSE IMPACT ENERGY BEFORE AND AFTER ELEVATED-TEMPERATURE EXPOSURE (6)

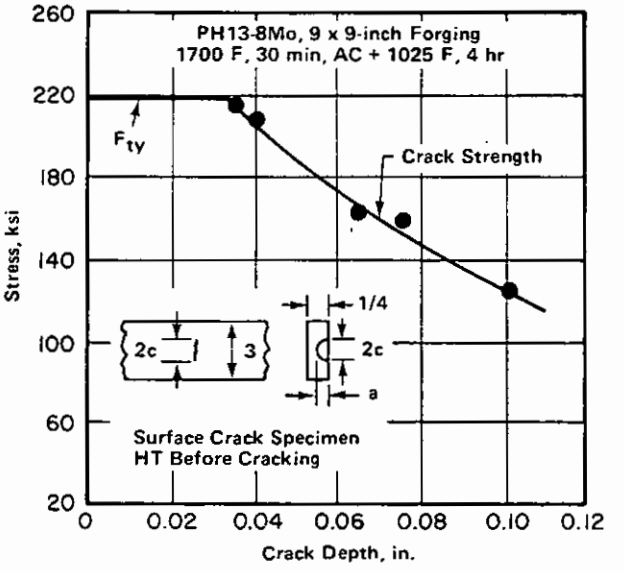

FIGURE 3.02711. EFFECT OF SURFACE CRACKS ON CRACK STRENGTH (12)

Alloy	PH13-8Mo	
Form	Bar	
Condition	H 950	H 1000
F_{sy}[a], ksi	137.1	134.0
F_{sty}, ksi	148.0	143.2
G, ksi	11.1×10^3	10.9×10^3
F_{st}, ksi	184.4	171.9

(a) Shear yield strength.

TABLE 3.0251. TORSION AND SHEAR PROPERTIES (3)

Alloy	PH13-8Mo			
Form	0.1-inch Sheet			
Condition	Test Direction	e/D	F_{bry}, ksi	F_{bru}, ksi
H 1000	L	1.5	290	330
		2.0	375	448
	T	1.5	300	340
		2.0	380	442

TABLE 3.0261. BEARING PROPERTIES OF SHEET IN CONDITION H 1000 (13)

Fe
13 Cr
8 Ni
2 Mo

PH13-8Mo

Alloy	PH13-8Mo	
Condition	H 1000	
	Forging Cross-Section Size, inch	
Form	6 x 21	5 x 24
Orientation	Plane Strain Fracture Toughness, K_{Ic}, ksi $\sqrt{in.}$	
TL	108	116
LT	–	115
		75[a]

Note: Testing procedure and data conform to ASTM E 399; data average of two or more tests; compact tension specimen; thickness, B, 1 inch.

(a) Test temperature – 65 F.

TABLE 3.02721. PLANE-STRAIN FRACTURE TOUGHNESS FOR CONDITION H 1000 (15)

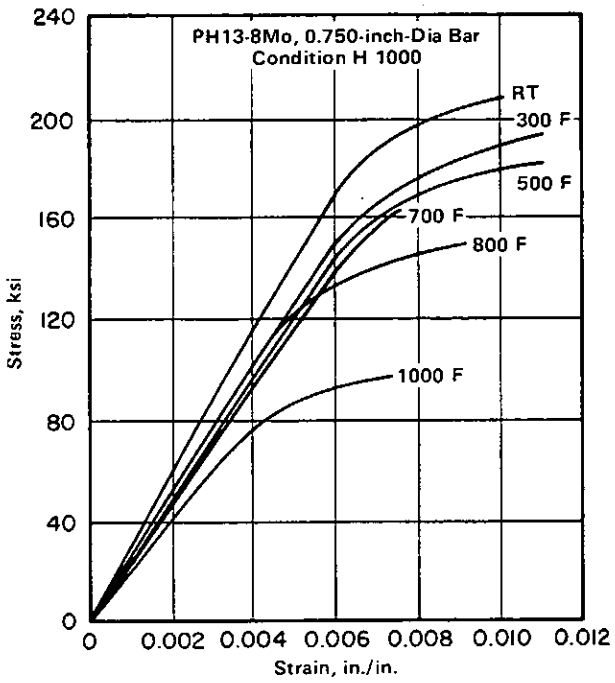

FIGURE 3.0311. STRESS-STRAIN CURVES AT ELEVATED TEMPERATURES FOR BAR IN CONDITION H 1000 (13)

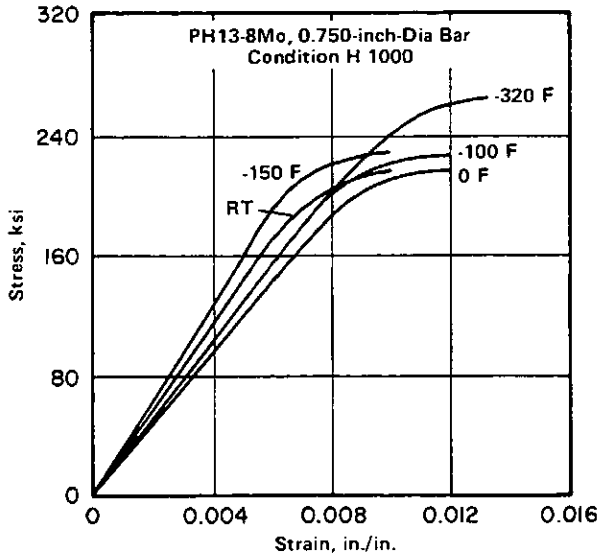

FIGURE 3.0312. STRESS-STRAIN CURVES AT ROOM AND LOW TEMPERATURE FOR BAR IN CONDITION H 1000 (13)

Fe
13 Cr
8 Ni
2 Mo

PH13-8Mo

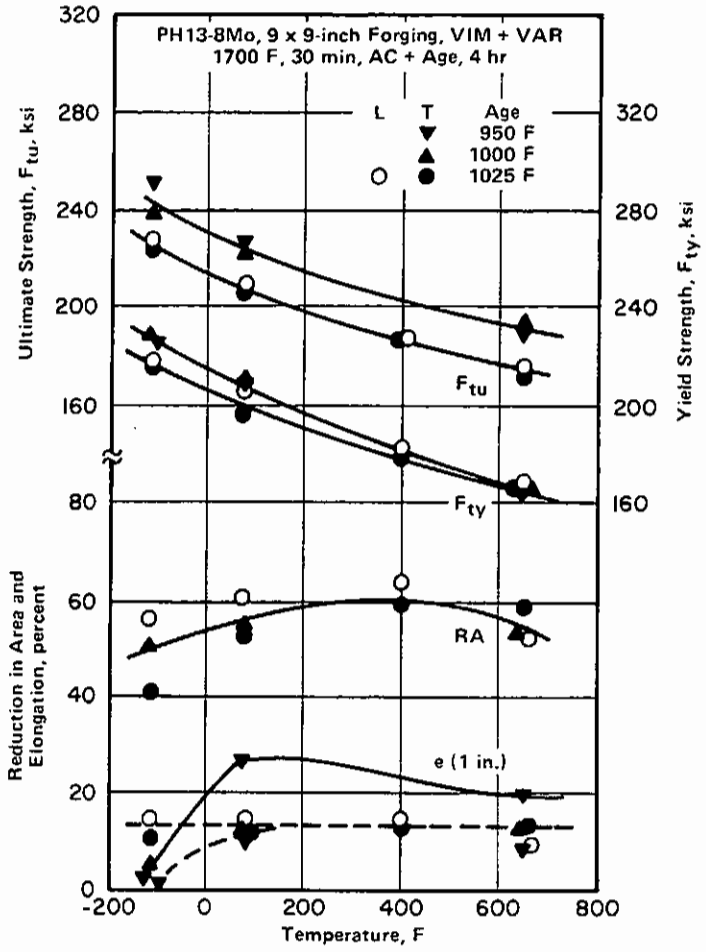

FIGURE 3.0313. EFFECT OF TEST TEMPERATURE ON TENSILE PROPERTIES OF A FORGING (12)

Alloy	PH13-8Mo					
Condition	H 1000					
Form	Forging					
Cross-Sectional Size, in.	Test Temp., F	Orientation	F_{tu}, ksi	F_{ty}, ksi	e (1 in.), percent	RA, percent
13 x 13	RT	L	212	205	14	60
		T	210	204	14	58
		ST	205	200	14	58
	-110	L	234	224	15	56
		T	230	218	16	51
		ST	230	216	15	50
4-1/2 x 4-1/2	RT	L	214	206	14	55
		T	218	210	14	55
	-110	L	235	229	14	53
		T	234	227	13	47
1-1/2 x 13	RT	L	208	202	14	60
		T	212	204	16	61
	-110	L	227	219	16	58
		T	234	226	14	58

Note: Data average of two tests.

TABLE 3.0314. EFFECT OF TEST TEMPERATURE AND ORIENTATION ON THE TENSILE PROPERTIES OF VARIOUS-SIZE FORGINGS (14)

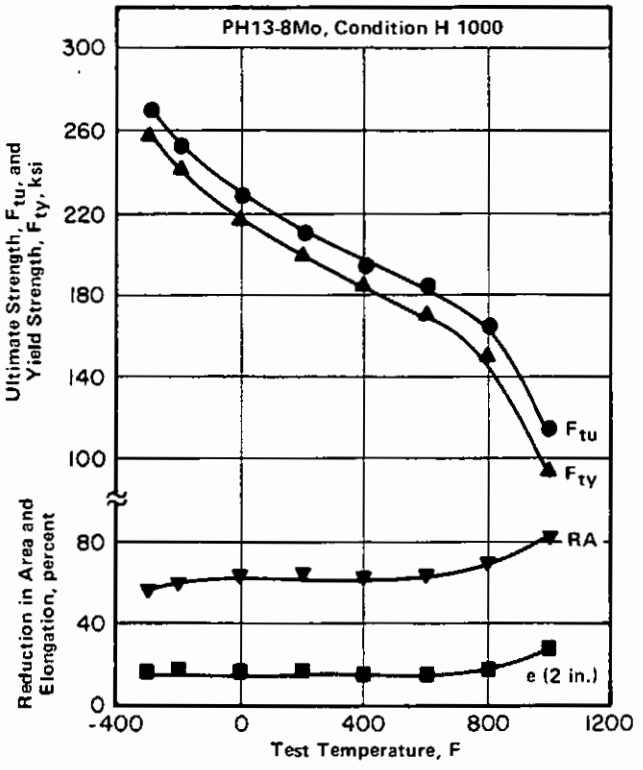

FIGURE 3.0315. TENSILE PROPERTIES OF BAR AT CRYOGENIC AND ELEVATED TEMPERATURES (22)

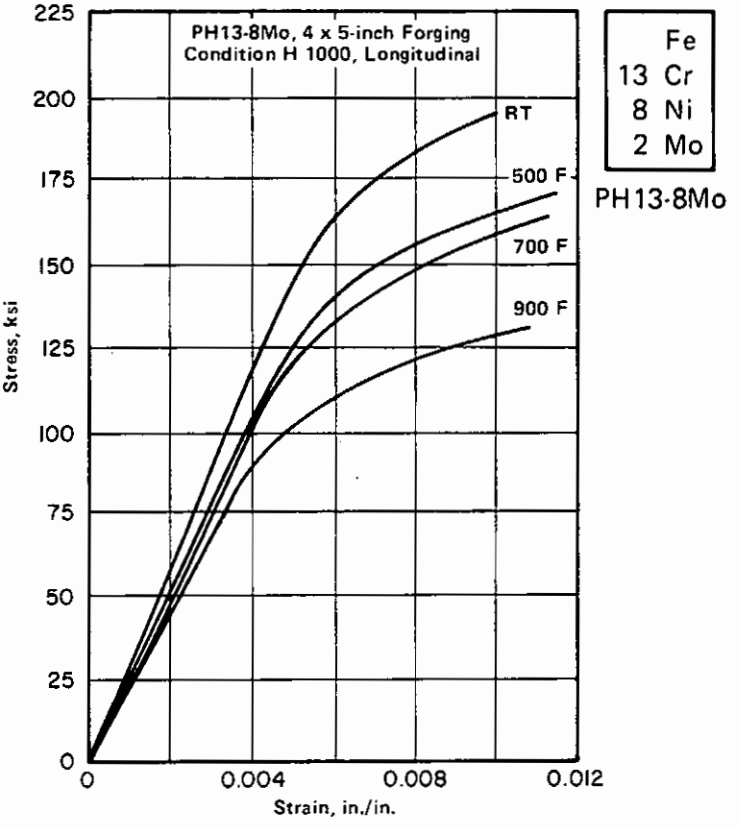

FIGURE 3.0321. STRESS-STRAIN CURVES FOR A FORGING IN COMPRESSION AT ELEVATED TEMPERATURES (17)

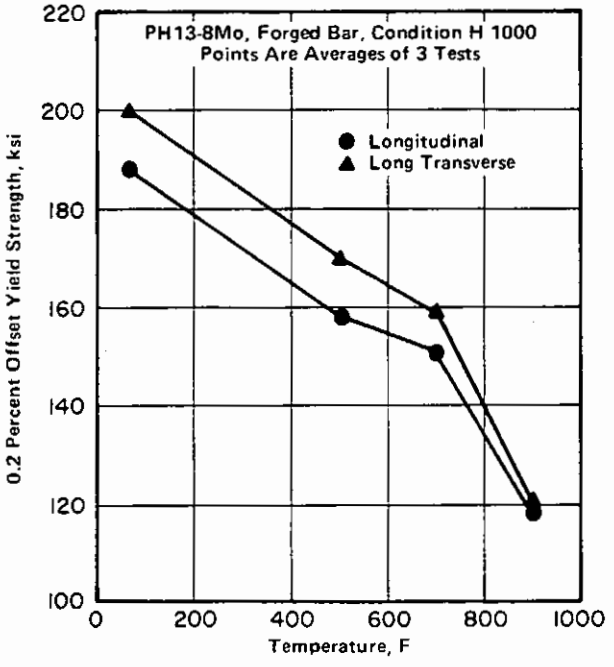

FIGURE 3.0322. EFFECT OF TEMPERATURE ON COMPRESSIVE YIELD STRENGTH (17)

Fe
13 Cr
8 Ni
2 Mo

PH13-8Mo

Alloy	PH13-8Mo				
Form	1-inch-Diameter Bar				
Condition	H 950	H 1000	H 1050	H 1100	H 1150-M
Test Temp., F	IE Charpy V, ft-lb				
RT	24	30	40	50	–
-32	11	20	35	46	–
-65	7	12	22	38	–
-110	5	8	13	32	88
-175	3	6	–	–	71
-220	2	5	6	14	–
-320	2	4	4	5	30

TABLE 3.0331. TYPICAL LOW-TEMPERATURE IMPACT ENERGIES OF BAR IN VARIOUS AGED CONDITIONS (3)

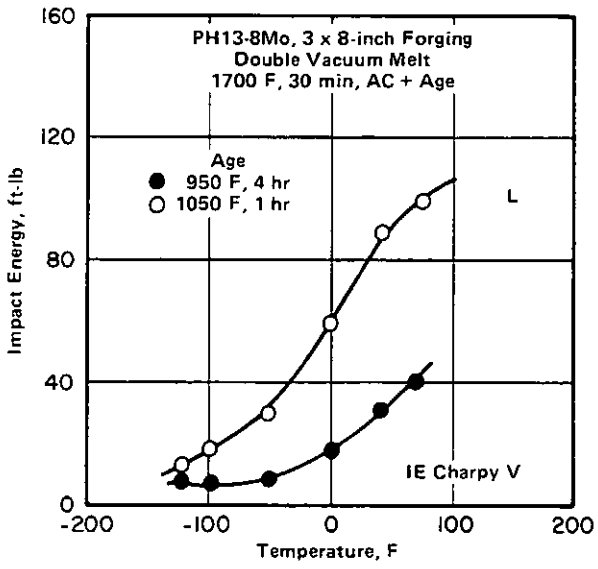

FIGURE 3.0332. EFFECT OF TEST TEMPERATURE ON IMPACT PROPERTIES OF A FORGING (6)

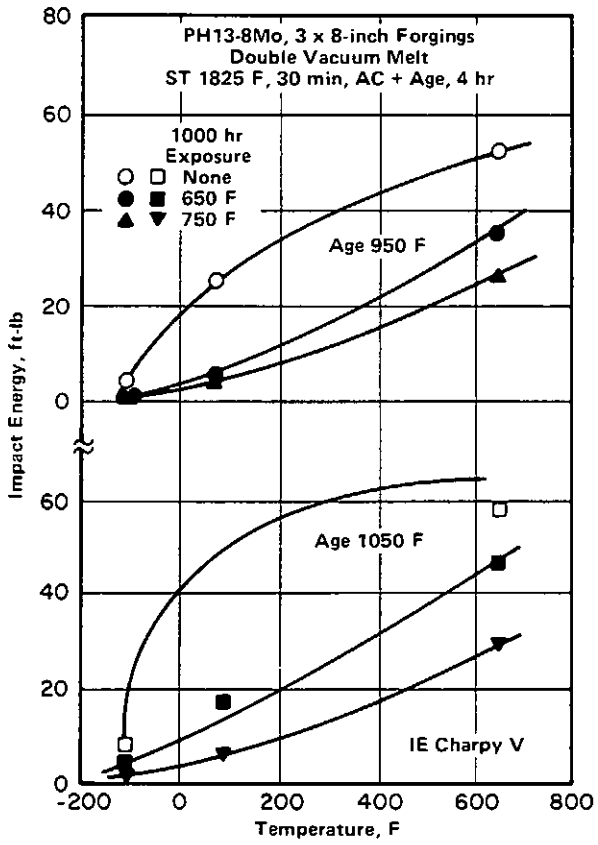

FIGURE 3.0333. EFFECT OF TEST TEMPERATURE AND EXPOSURE TEMPERATURE ON THE IMPACT ENERGY OF FORGINGS (6)

Fe
13 Cr
8 Ni
2 Mo

PH13-8Mo

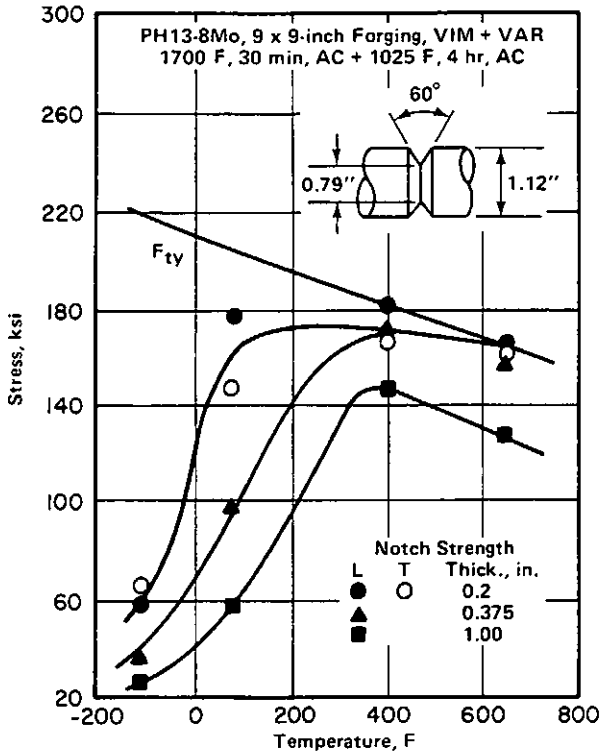

FIGURE 3.03711. EFFECT OF TEST TEMPERATURE ON SHARP NOTCH STRENGTH OF A FORGING (12)

Alloy	PH13-8Mo				
Form	0.75-inch-Diameter Bar				
Condition	H 1000				
Test Temp., F	Stress Concentration Factor, K_t	F_{ty}, ksi	F_{tu}, ksi	NTS, ksi	NTS/F_{tu}
80	3.8	212	220	355	1.61
	5.25	212	220	347	1.57
-110	3.8	–	235	384	1.64
	5.25	–	235	373	1.59

Notched Round Bar

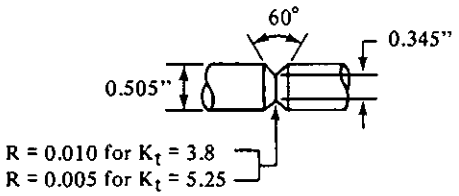

TABLE 3.03712. EFFECT OF STRESS-CONCENTRATION FACTOR ON TENSILE AND NOTCH PROPERTIES OF BAR AT ROOM AND LOW TEMPERATURE (3)

Fe
13 Cr
8 Ni
2 Mo
PH13-8Mo

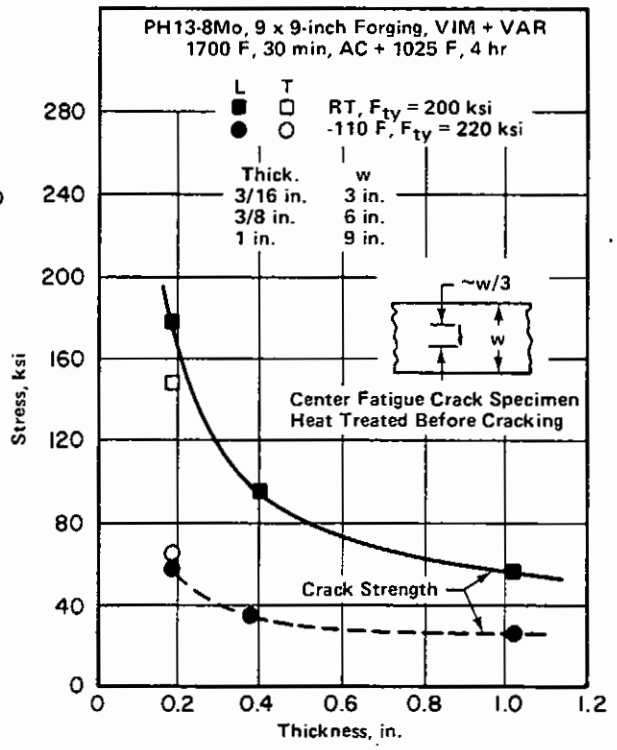

FIGURE 3.03713. EFFECT OF THICKNESS ON CRACK STRENGTH OF A FORGING AT ROOM AND LOW TEMPERATURE (12)

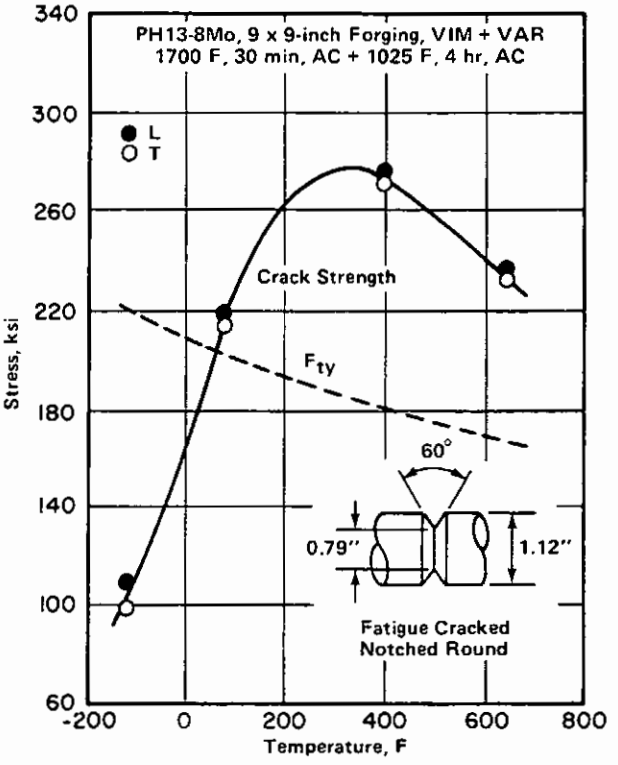

FIGURE 3.03714. EFFECT OF TEST TEMPERATURE ON CRACK STRENGTH OF A FORGING (12)

Alloy	PH13-8Mo		
Condition	H 1000		
Test Temp.	-110 F		
Form	Forging Cross-Sectional Size, inch		
	13 x 13	4-1/2 x 4-1/2	1-1/2 x 13
Orientation	Plant Strain Fracture Toughness, K_{Ic}, ksi $\sqrt{in.}$		
LT	53	43	47
TL	56	41	47

Note: Testing procedure and data conform to ASTM E 399. Data average of two or more tests. Single-edge crack specimen: thickness, B, 0.5 inch.

TABLE 3.03721. PLANE-STRAIN FRACTURE TOUGHNESS OF A FORGING AT LOW TEMPERATURE (14)

Fe
13 Cr
8 Ni
2 Mo
PH13-8Mo

Alloy	PH13-8Mo			
Form	Condition	Test Temperature, F	Specimen Orientation	Fracture Toughness[a], K_{Ic}, ksi $\sqrt{in.}$
Upset forging	H 1000	70	TL	82 (1)
			ST	86 (1)
		-65	LT	53 (2)
Forged bar	H 1000	70	LT	98 (5)
			TL	91 (3)
		-65	TL	55 (2)
Extruded bar	Re-solution + H 1000	70	LT	74 (3)
Rolled bar	H 1000	70	LT	89 (4)
			TL	75 (2)
		-65	LT	50 (4)
	RH 950	70	LS	60 (4)
	RH 975	70	LS	70 (3)
	RH 1000	70	LS	95 (1)

(a) Values averaged from number of specimens in parentheses.

TABLE 3.03722. FRACTURE TOUGHNESS OF VARIOUS WROUGHT FORMS AT ROOM AND CRYOGENIC TEMPERATURES (31)

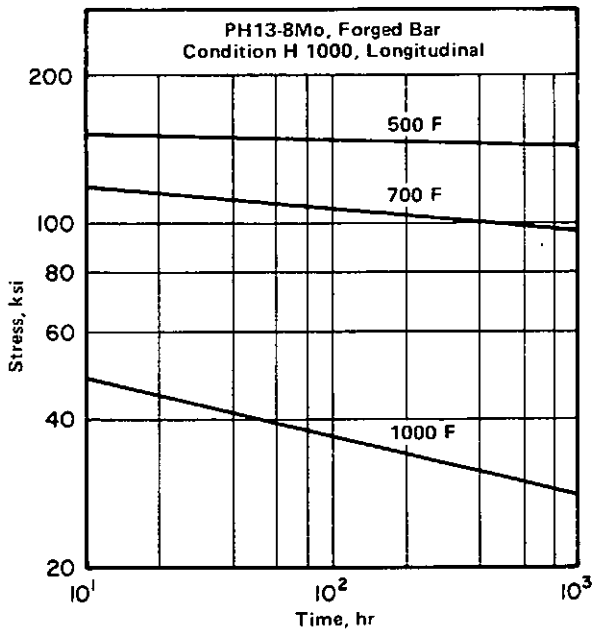

FIGURE 3.041. TIME TO 0.2 PERCENT CREEP DEFORMATION FOR BAR AT ELEVATED TEMPERATURES (32)

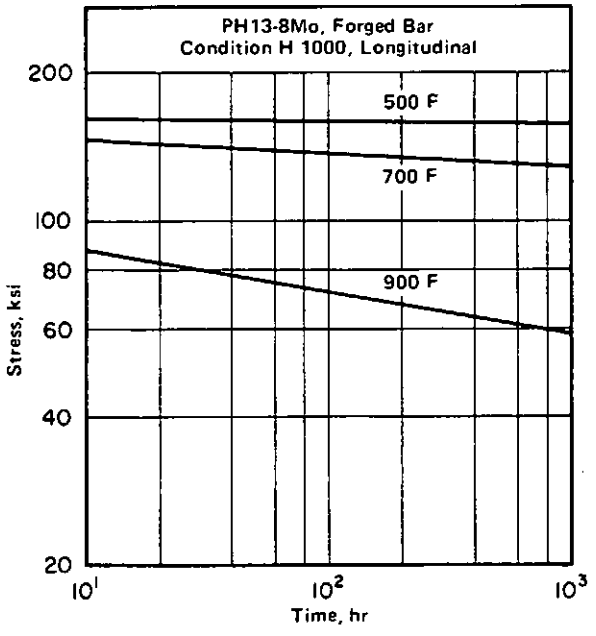

FIGURE 3.042. TIME TO RUPTURE FOR BAR AT ELEVATED TEMPERATURES (32)

Fe
13 Cr
8 Ni
2 Mo

PH13-8Mo

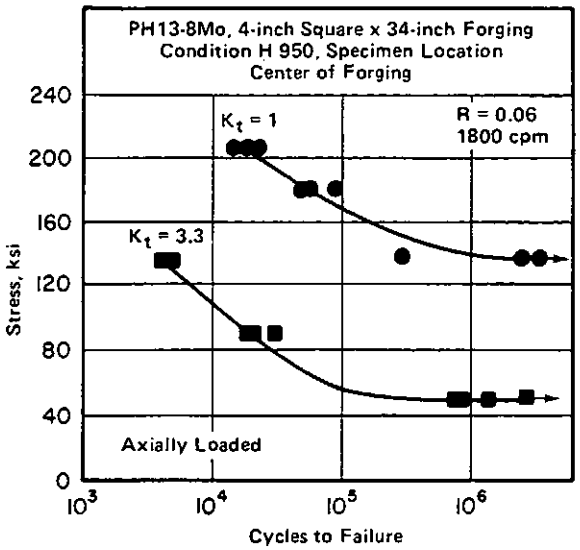

FIGURE 3.051. EFFECT OF STRESS CONCENTRATIONS ON FATIGUE STRENGTH OF A FORGING (16)

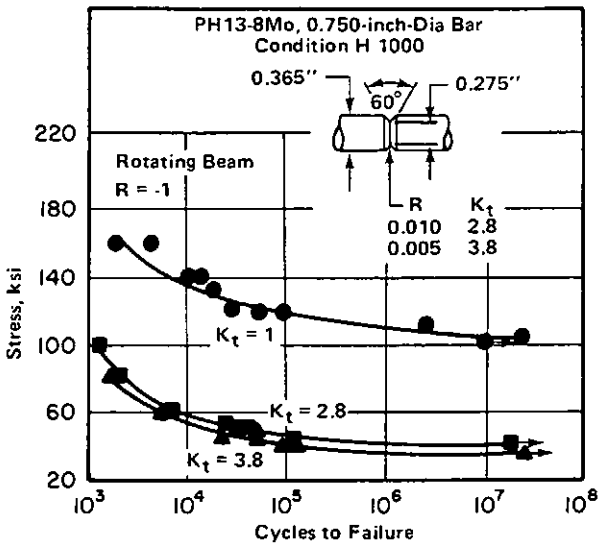

FIGURE 3.052. S-N CURVES FOR SMOOTH AND NOTCHED SPECIMENS OF BAR (3)

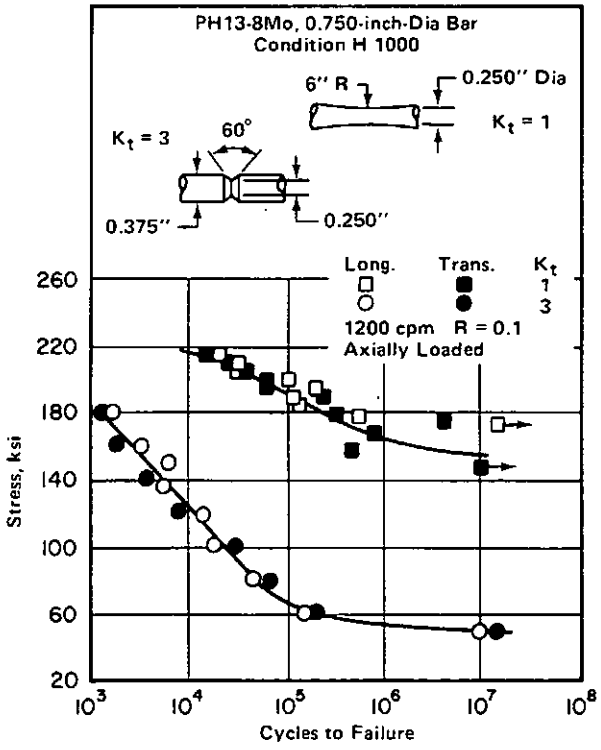

FIGURE 3.053. S-N CURVES FOR LONGITUDINAL AND TRANSVERSE SMOOTH AND NOTCHED SPECIMENS FROM BAR AT A STRESS RATIO OF R = 0.1 (3)

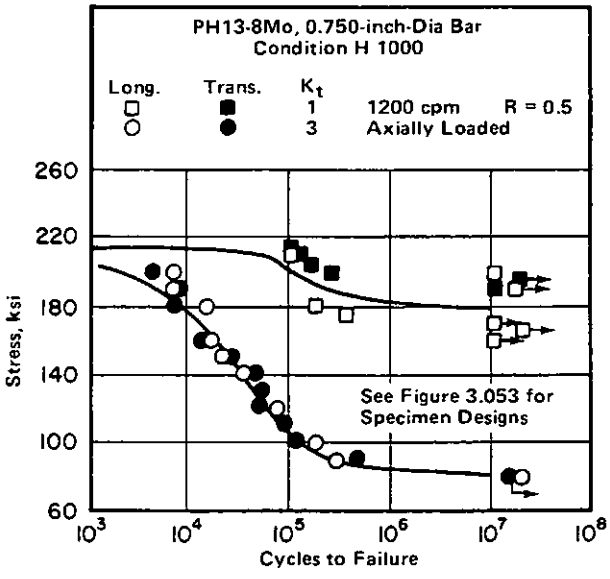

FIGURE 3.054. S-N CURVES FOR LONGITUDINAL AND TRANSVERSE SMOOTH AND NOTCHED SPECIMENS FROM BAR AT A STRESS RATIO OF R = 0.5 (3)

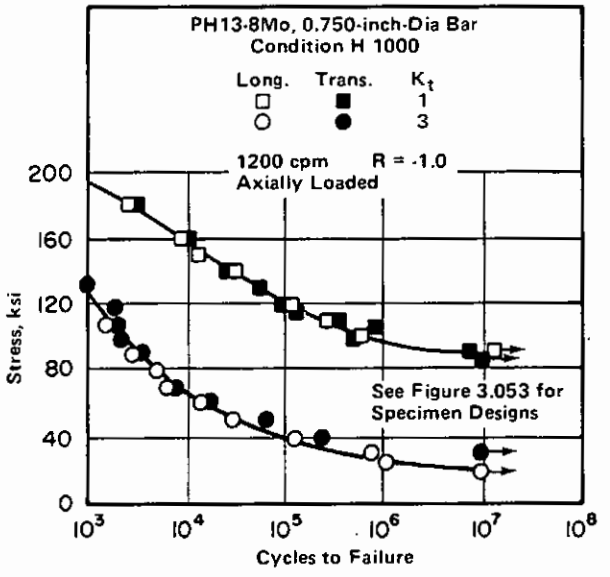

FIGURE 3.055. S-N CURVES FOR LONGITUDINAL AND TRANSVERSE SMOOTH AND NOTCHED SPECIMENS FROM BAR AT A STRESS RATIO OF R = -1.0 (3)

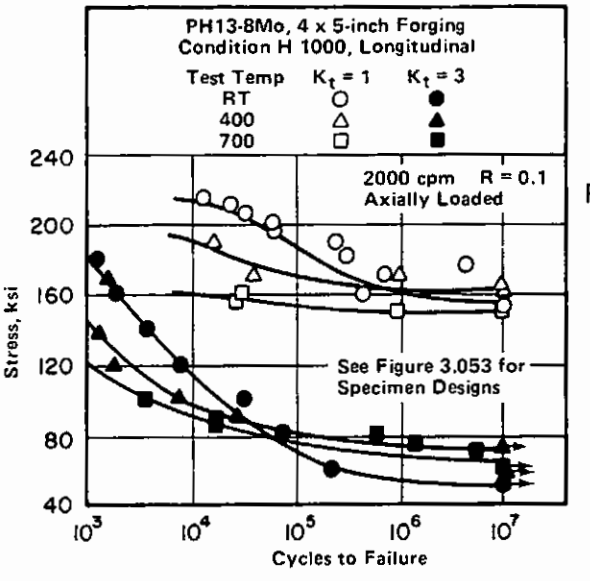

Fe
13 Cr
8 Ni
2 Mo

PH13-8Mo

FIGURE 3.056. S-N CURVES AT ELEVATED TEMPERATURES FOR LONGITUDINAL SMOOTH AND NOTCHED SPECIMENS FROM A FORGING AT A STRESS RATIO OF R = 0.1 (17)

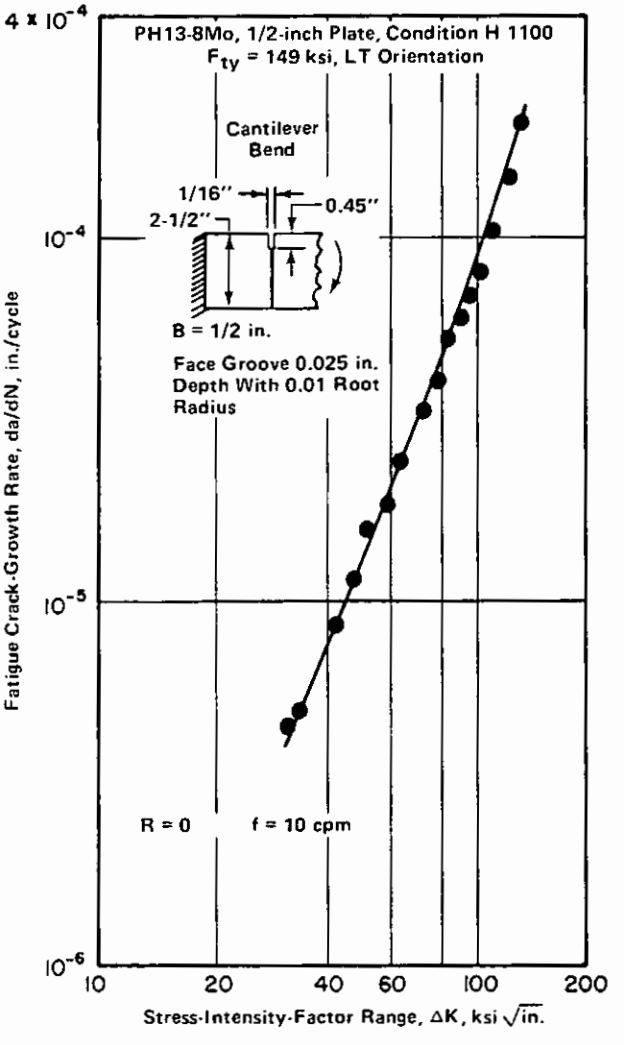

FIGURE 3.057. FATIGUE CRACK-GROWTH RATE AT ROOM TEMPERATURE FOR PLATE (18)

Fe
13 Cr
8 Ni
2 Mo

PH13-8Mo

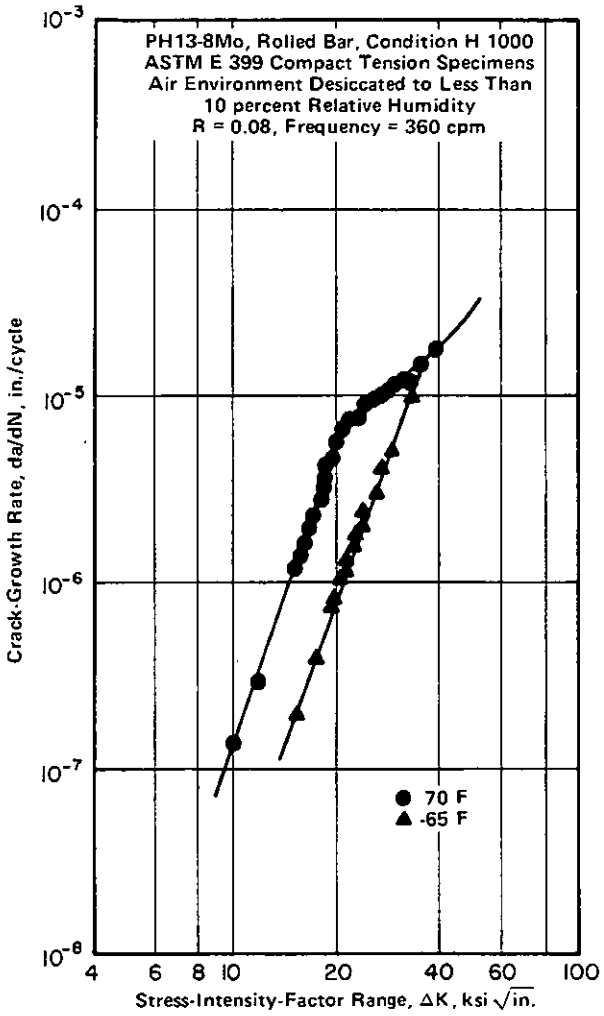

(a) LT Orientation

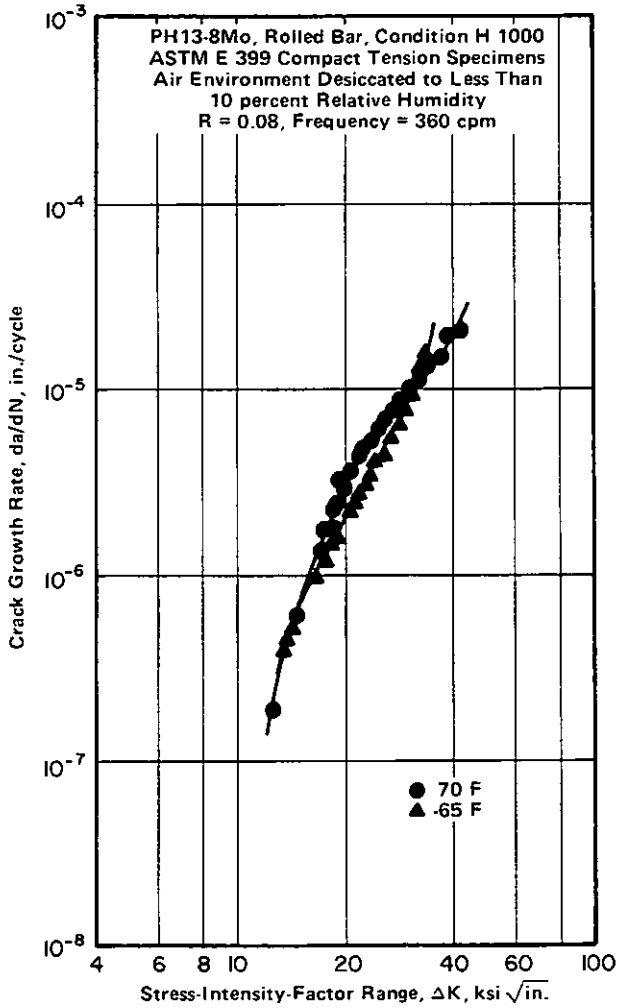

(b) TL Orientation

FIGURE 3.059. FATIGUE CRACK-GROWTH RATE IN LOW-HUMIDITY AIR AT LOW TEMPERATURES (31,33)

Fe
13 Cr
8 Ni
2 Mo
PH13-8Mo

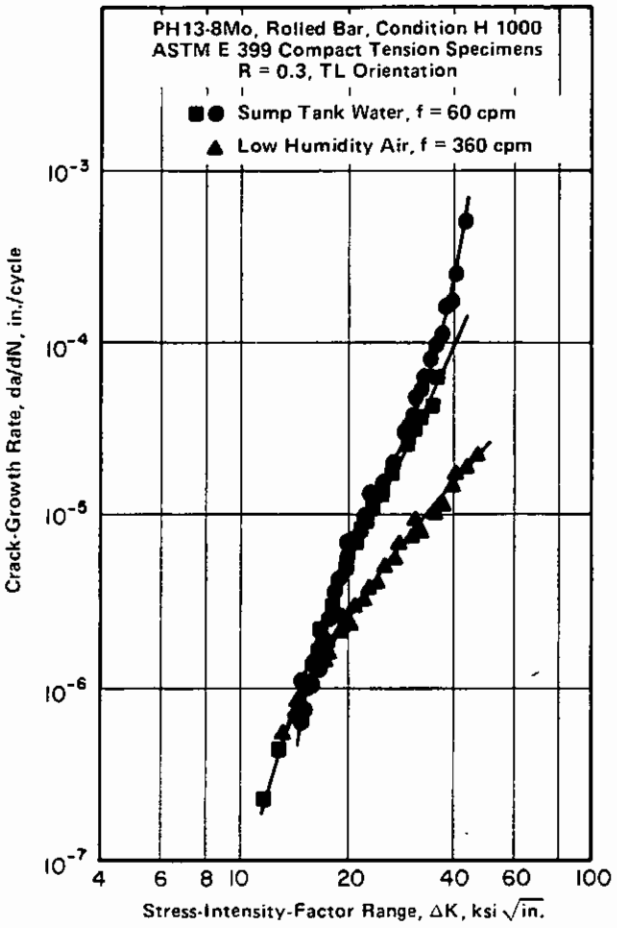

FIGURE 3.0510. FATIGUE CRACK-GROWTH RATE IN FUEL-TANK SUMP WATER AND IN AIR AT ROOM TEMPERATURE (31,33)

Alloy	PH13-8Mo			
Form	0.750-inch-Diameter Bar			
Condition	H 950	H 1000	H 1050	H 1100
E, ksi x 10^3	28.6	32.0	30.8	28.6

TABLE 3.0621. TENSILE MODULUS OF BAR IN VARIOUS AGED CONDITIONS (13)

Fe
13 Cr
8 Ni
2 Mo

PH13-8Mo

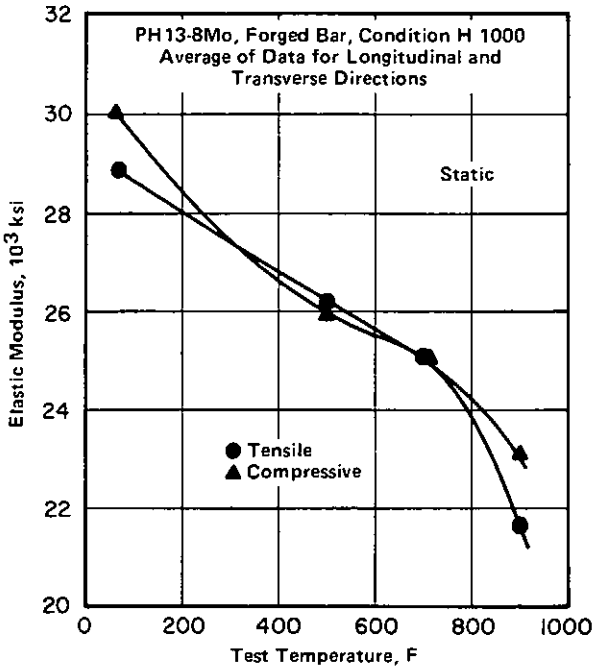

FIGURE 3.0622. ELASTIC MODULI OF FORGED BAR IN TENSION AND COMPRESSION AT ROOM AND ELEVATED TEMPERATURES (32)

Alloy	PH13-8Mo		
Form	3 x 3-inch Forging		
Condition	BCHT 950(a)		
Direction	L	T	ST
F_{tu}, ksi	226	223	224
F_{ty}, ksi	207	200	199
e (1 in.), percent	13	15	17
RA, percent	66	63	61
Charpy V, ft-lb	22	–	–
Hardness, HRC	47	–	–

(a) Specimen blanks were cut and then heat treated.

TABLE 4.0131. TENSILE AND IMPACT PROPERTIES OF FORGINGS SUBJECTED TO A BRAZE-CYCLE HEAT TREATMENT (5)

Alloy	PH13-8Mo											
Form	Plate											
	Tensile Properties at Indicated Plate Thickness, inch											
	F_{tu}, ksi			F_{ty}, ksi			e, percent			RA, percent		
Condition(a)	0.187	0.50	0.75	0.187	0.50	0.75	0.187	0.50	0.75	0.187	0.50	0.75
Unwelded base plate + H 950	220	232	225	204	214	208	12	17	16	–	63	62
Weld + H 950	215	207	195	203	173	160	10	14	13	–	51	47
Weld + Condition A + H 950	216	217	213	203	203	195	10	9	18	–	26	20
Unwelded base plate + H 1000	214	216	160	200	210	132	13	17	22	–	65	71
Weld + H 950	204	200	152	199	163	94	11	14	20	–	61	70
Weld + Condition A + H 1000	201	210	147	197	205	96	11	9	20	–	37	60
Unwelded base plate + H 1100	–	173	–	–	163	–	–	22	–	–	71	–
Weld + H 1100	–	165	–	–	124	–	–	18	–	–	71	–
Weld + Condition A + H 1100	–	162	–	–	158	–	–	8(b)	–	–	29(b)	–

(a) Welding conditions: GTA (gas tungsten arc) weld process; base plate welded in Condition A; filler metal was WPH13-8Mo.
(b) Low-ductility values resulted from incomplete weld penetration.

TABLE 4.034. EFFECT OF HEAT TREATMENT ON THE MECHANICAL PROPERTIES OF WELDMENTS AS A FUNCTION OF PLATE THICKNESS (3,34)

Fe
13 Cr
8 Ni
2 Mo
PH13-8Mo

Alloy	PH13-8Mo			
Weld Type	Postweld Stress Relief	Notch Location	Test Temperature, F	Fracture Toughness[a], K_{Ic}, ksi $\sqrt{in.}$
Butt weld	2 hr, 950 F	HAZ	70	88 (4)
			-65	95 (2)
		Weld	70	83 (1)
			-65	98 (1)
	4 hr, 1000 F	HAZ	70	93 (2)
Weld overlay	None	Weld	70	83 (1)
	2 hr, 950 F	Weld	70	79 (1)

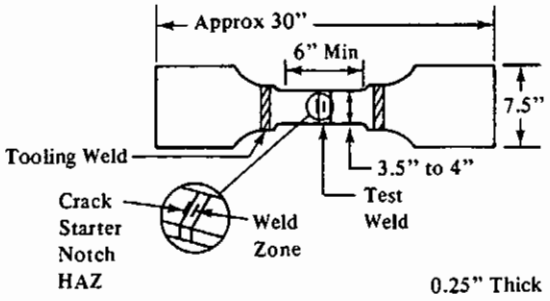

(a) Value averaged from number of specimens in parentheses. These are conditional values based on data from part-through-cracked specimens.

TABLE 4.037. FRACTURE TOUGHNESS OF WELDED MATERIAL AT ROOM AND CRYOGENIC TEMPERATURES (31)